# Chapitre 3

# Diminution de la productivité biologique lors des périodes glaciaires déduite de l'étude du rapport $(^{231}Pa/^{230}Th)_{xs,0}$ dans les sédiments marins de l'océan Pacifique équatorial

# Lower Biological Productivity During Glacial Periods in the Equatorial Pacific as derived from $(^{231}Pa/^{230}Th)_{xs,0}$ Measurements in Deep-sea Sediments

Sylvain Pichat[1], Ken W. Sims[2], Roger François[2], Jerry F. McManus[2], Francis Albarède[1]

[1] Laboratoire de Sciences de la Terre, Ecole normale supérieure de Lyon, 46, allée d'Italie, F-69364 Lyon cedex 7, France

[2] Woods Hole Oceanographic Institution, Woods Hole, MA 02543, U.S.A.

*In preparation*

## Abstract

Measurements of the $(^{231}Pa/^{230}Th)_{xs,0}$ ratio have been carried out by SF-ICP-MS for three deep-sea sediment cores collected in the equatorial Pacific. They reveal systematically lower values during glacial periods over the last 85,000 years. An enhanced particle flux in the whole Pacific cannot account for the whole variations observed. Hence a lower productivity during glacial periods is inferred, which apparently contradicts previous conclusions deduced from carbonate, organic carbon and barite accumulation rates in the eastern equatorial Pacific. The use of $(^{230}Th)_{xs,0}$ normalized fluxes instead of $\delta^{18}O$-derived accumulation rates show that the carbonate and barite normalized fluxes vary insignificantly between glacial and interglacial periods. The higher $\delta^{18}O$-derived accumulation rates can be related to enhanced sediment focusing during glacial periods. New Guinea is the main source of iron for the equatorial Pacific via the export along the equatorial undercurrent. The lower glacial productivity inferred

from our measurements could arise from lower iron input from New Guinea as a consequence of glacial sea level stand. When combined with enhanced upwelling rates, this lower productivity would have caused enhanced $CO_2$ transfer from the ocean to the atmosphere during glacial periods in the equatorial Pacific, which therefore have to be taken into account into the models of atmospheric $CO_2$ draw down during glacial periods.

# 1 - Introduction

One of the more spectacular datasets for Quaternary climatology has been derived from the analysis of gas bubbles trapped in the polar ice sheet which record a systematic lowering in the atmospheric $CO_2$ concentration during glacial periods (Neftel et al., 1982; Barnola et al., 1987). The atmospheric partial pressure of $CO_2$ at the Last Glacial Maximum (LGM, about 18,000 years ago) was lower by 30-40 % compared with the recent pre-industrial levels (interglacial period, roughly the last 12,000 years), i.e. 180-200 part per million by volume (ppmv) instead of 280-290 ppmv for the climatically relatively stable pre-industrial Holocene. $CO_2$ is a major greenhouse gas, and therefore variations in the atmospheric $CO_2$ concentration are thought to cause major modifications in the climate of the Earth either as a cause or a feedback. Consequently, the study of the carbon cycle is essential to understand climate variability between glacial and interglacial periods.

Mass balance and residence times considerations on the carbon reservoirs clearly point to the deep ocean as the primary modulator of the $CO_2$ budget (Siegenthaler and Sarmiento, 1993; Holmen, 1992; Sigman and Boyle, 2000). The $CO_2$ storage capacity of the ocean is a function of both global circulation and biochemical processes. The biological pump is the mechanism of transfer of organic carbon by sinking biogenic detritus from the surface ocean, where biological production occurs, to the deep ocean (Berger, 1989). An increase in productivity would increase the efficacy of this pump and allow more organic carbon to be buried into the deep-sea sediments and inorganic carbon

to be stored in the deep-ocean. As a result, the chemical composition and the nutrient content of the ocean could be changed.

Nutrients and inorganic $CO_2$ are brought back to the surface in upwelling zones. Consequently, the partial pressure of $CO_2$ and the nutrient content in waters located in upwelling zones are higher than in the rest of the ocean. In these zones two competitive phenomena are involved. The high nutrient content leads to a high primary productivity. Consequently, the biological pump is very efficient in removing organic carbon from the surface ocean, thus allowing more $CO_2$ to be transferred from the atmosphere into the ocean. The upwelling of inorganic carbon enriched waters competes with the biological pump in increasing the surface waters carbon content, therefore increasing the leak of $CO_2$ from the surface waters to the atmosphere. Currently, a net flux of $CO_2$ from the ocean to the atmosphere is observed in upwelling regions like the central and the eastern equatorial Pacific (Dandonneau, 1995; Boutin and Etcheto, 1997; Emerson et al., 1997). Variations in biological productivity, probably associated with changes in nutrient content of the oceans, is expected to influence the distribution of carbon between the atmosphere-upper ocean and the upper-lower oceans systems (Sigman and Boyle, 2000).

A number of proxies have previously been used to monitor productivity variations in the oceans: organic carbon (Müller and Suess, 1979), biogenic opal (Nelson et al., 1995), and biogenic barite (Dehairs et al., 1980) contents; calcium carbonate (Lyle et al., 1988; Isern, 1991; Wefer et al., 1999), organic carbon (Pedersen, 1983; Lyle et al., 1988; Isern, 1991), Al excess (Murray and Leinen, 1996, Murray et al., 1993), and barite (Paytan et al., 1996) accumulation rates. Microfossil assemblages (Vincent and Berger, 1981; Beaufort et al., 1997; Loubere, 1999) have also been widely employed. All these proxies must fulfill several conditions to be adequately used as paleoproductivity proxy. For example, the use of biogenic opal is not appropriate for the Pacific because the biogenic opal sediment content in this area is neither correlated to the particle flux nor to the surface productivity (Lange and Berger, 1993). Except for Al excess accumulation rates, all these proxies have in common their sensitivity to remineralization in both the water column and the sediment. These proxies are also affected by dilution by other phases and are sensitive to sediments remobilisation by bottom currents. Variability in the intensity of these phenomena could markedly affect the accuracy of the proxies.

At the beginning of the 90's, it was proposed that the ($^{231}$Pa/$^{230}$Th) excess activity ratio decay corrected to the time of deposition, referred hereafter to as ($^{231}$Pa/$^{230}$Th)$_{xs,0}$, has been proposed as a proxy to assess changes in biological productivity of the ocean during the last 150-200,000 years (Lao et al., 1992a,b; Kumar et al., 1993; 1995; Francois et al., 1993). The advantage of the ($^{231}$Pa/$^{230}$Th)$_{xs,0}$ ratio, over the abovementioned productivity proxies, is its insensitivity to remineralization, dilution, and sediment remobilization. The conditions required to use the ($^{231}$Pa/$^{230}$Th)$_{xs,0}$ ratio as a productivity proxy are met together in the Pacific ocean. They are detailed in the next section. As yet, only a few studies (Lao et al., 1992a, b; Stephens and Kadko, 1997) have been performed with Pacific materials to investigate productivity variations during the Quaternary.

We have focused our study on the equatorial Pacific because of the importance of this ocean in the dynamics of the Earth's climate (Cane 1998; Clement et al., 1999; Lea et al., 2000) as well as the need to understand long term variations in primary production at low latitudes (Thunell et al., 1994). The data coverage in the equatorial Pacific remains patchy. To better understand the contribution of this region to climate dynamics, we have measured the activity ratio of $^{231}$Pa excess to $^{230}$Th excess in three cores along the Equator in an effort to test the accuracy of the ($^{231}$Pa/$^{230}$Th)$_{xs,0}$ ratio as a paleoproductivity proxy and to reconstruct the glacial/interglacial productivity variations.

# 2 - The use of ($^{231}$Pa/$^{230}$Th)$_{xs,0}$ to determine biological paleoproductivity

## 2.1 - Theory

Uranium is homogeneously distributed in the ocean because of its long residence time, $\tau_U$=200-450,000 years (Brewer, 1975; Ku et al., 1977; Chen et al., 1986), compared with the mixing time of the ocean, $t_{mix}$=1,000-1,600 years (Broecker and Peng,

1982), and the absence of strong biolimiting processes. As a consequence, $^{231}Pa$ ($t_{1/2}$ = 32,760 years) and $^{230}Th$ ($t_{1/2}$ = 75,380 years) (Firestone, 1996) are uniformly produced, at a constant rate, in the water column, from α-decay of $^{234}U$ and $^{235}U$ respectively with an initial activity ratio of 0.093, referred hereafter as the production ratio. Unlike uranium, both nuclides are extremely reactive to particles, which leads to residence times in the water column of 10-40 years for $^{230}Th$ (Brewer et al., 1980; Nozaki et al., 1981; Huh and Beasley, 1987) and 50-200 years for $^{231}Pa$ (Anderson et al., 1983b; Nozaki and Nakanishi, 1985; Yu et al., 1996). As a consequence, the radioactive decay of the two radionuclides in the water column can be neglected because their residence times are short relative to their half-lives. Furthermore, their difference in particle reactivity lead to fractionation between $^{230}Th$ and $^{231}Pa$. $^{230}Th$ is almost totally scavenged from the water column by the vertical particle flux (Bacon and Rosholt, 1982; Anderson et al., 1983a,b; Bacon, 1984; François et al., 1990), whereas dissolved $^{231}Pa$, because of its lower particle affinity, can be laterally transported over oceanic basin scale distance. Consequently, $^{231}Pa$ is preferentially removed in areas of high vertical particle flux (Anderson et al., 1983b; Yu et al., 1996; Bacon, 1988), resulting in $(^{231}Pa/^{230}Th)_{xs,0} > 0.093$ in sediments. This process is called “boundary scavenging” as it occurs mostly at ocean margins (Yang et al., 1986; Anderson et al, 1983b, Shimmield et al., 1986). It is the main cause of regional variability in the $(^{231}Pa/^{230}Th)$ ratio of sediments within ocean basins. As a result of this positive relationship between mass flux of particles and export productivity (Deuser et al., 1981; Betzer et al., 1984, Yu et al., 1994), it has been proposed that the $(^{231}Pa/^{230}Th)_{xs,0}$ ratio can be used as a paleoproductivity proxy (Lao et al., 1992b; Kumar et al., 1993).

## 2.2 - Required environmental conditions to use $(^{231}Pa/^{230}Th)_{xs,0}$ as a paleoproductivity proxy

For $^{231}Pa$, two conditions are required for effective boundary scavenging to occur (Lao et al., 1992b; Walter et al., 1999). (1) There must be a horizontal gradient in the dissolved radionuclides concentration, i.e., there must be an area where the

scavenging rate is high compared with the rest of the basin. This gradient will allow the transport of radionuclides by eddy diffusion to the area of higher particle flux. (2) The residence time of the radionuclide in the water column must be longer than the lateral diffusive mixing time of the basin, so that a significant amount of the radionuclide produced in the low particle flux regions can be transported to the high flux region.

The chemical composition of the sinking particles and its temporal variations control the fractionation between protactinium and thorium in the oceans. The fractionation factor, referred hereafter as F, defined as the ratio between the partition coefficients ($K_d$) of $^{231}$Pa and $^{230}$Th between the particulate and the dissolved phases ($F = (A^{230}Th/A^{231}Pa)_p/(A^{230}Th/A^{231}Pa)_d = K_{d,230Th} / K_{d,231Pa}$, where A, p, and d denote the activity, particulate, and dissolved phase, respectively). The value of F is around 10 in open ocean (Anderson et al., 1983a, Nozaki and Nakanishi, 1985; Walter et al., 1997). Anderson and co-workers (1992) have shown experimentally that particulate hematite, silica and manganese dioxide do not substantially fractionate the thorium and the protactinium, with F values of 2.1, 1.1, and 0.8, respectively. The presence of $MnO_2$ coated particles, originating from the recycling of reduced Mn from suboxic sediments, leads to an enhanced scavenging of $^{231}$Pa relative to $^{230}$Th, at ocean margins in the Panama and Guatemala Basins (Anderson et al., 1983b) or near the coast of Baja California (Shimmield et al., 1986). The estimated fractionation factors in this area range from 6.1 to 0.49 (Anderson et al., 1983b). Studies in sediment cores located near hydrothermal vents, which are important localized sources of Mn and Fe oxides, support the same conclusion (Kadko, 1980; Shimmield and Price, 1988). Shimmield and Price (1988) and Frank et al. (1994) have also shown intensified $^{230}$Th and $^{231}$Pa scavenging during pulsed hydrothermal activity. Finally, in areas where particle fluxes have a high biogenic opal content, like in the Southern Ocean, F values range between 1.12 and 3.3 (Walter et al., 1997; Walter et al., 2001). Accordingly, the $(^{231}Pa/^{230}Th)_{xs,0}$ ratio cannot be used as a paleoproductivity proxy near hydrothermal vents and in zones where the nature of the settling particles varies through time. For the Pacific, such areas are the East Pacific Rise and some coastal basins, e.g. the Baja, Guatemala, and Panama basins. The conditions required for a proper use of the $(^{231}Pa/^{230}Th)_{xs,0}$ ratio as a productivity proxy have to be tested for each specific location.

## 2.3 - Flux normalization to $^{230}Th_{xs,0}$ and focusing factor

Resuspension and sediments advection by bottom current leads to focusing or winnowing. In areas of highly dynamic hydrographical bottom regime, lateral supply of particles can exceed the vertical particle flux by a factor of up to 20 (Francois et al., 1990, 1993). The equatorial Pacific is not characterized by very dynamic bottom currents, none the less, the rain rates must be corrected for focusing or winnowing (Broecker et al., 1999; Higgins et al., 1999).

The flux of $^{230}Th_{xs,0}$ is assumed to be equal within 10-30 % to its local production rate in the water column (Frank et al., 1999; Henderson et al., 1999). Therefore vertical particle flux unaffected by sediment redistribution can be reconstructed by normalizing the flux of each component to $^{230}Th_{xs,0}$ (Suman and Bacon, 1989). The total normalized flux, or "true" rain rate, referred hereafter as *RR*, is given by:

$$RR = \frac{\beta z}{(^{230}Th_{xs,0})} \quad (1)$$

and the normalized flux for a component i, designated hereafter as $RR_i$, is given by:

$$RR_i = \frac{\beta z f_i}{(^{230}Th_{xs,0})} \quad (2)$$

where $\beta$ is the constant production rate of $^{230}Th$ from $^{234}U$ in the water column ($\beta$ = 2.63 dpm $cm^{-2}$ $kyr^{-1}$ per km of water depth), $z$ is the water depth (in km), ($^{230}Th_{xs,0}$) is the activity of $^{230}Th$ in excess corrected to the time of deposition (in dpm/$g_{sediment}$), $f_i$ is the weight fraction of component *i*.

The focusing factor, referred hereafter to as $\psi$, has been defined by Suman and Bacon (1989) as the ratio between the expected rain rate of $^{230}Th_{xs,0}$ deduced from the decay of $^{234}U$ in the water column, i.e. $\beta z$, to the observed rain rate of $^{230}Th_{xs,0}$:

$$\psi = \frac{\int_{z_1}^{z_2} (^{230}Th_{xs,0})\rho_r dr}{\beta z(t_1 - t_2)} \quad (3)$$

where $\rho_r$ is the average dry bulk density (in g $cm^{-3}$) between horizons 1 and 2, ($^{230}Th_{xs,0}$) is the average activity of $^{230}Th$ in excess corrected to the time of deposition (in $dpm/g_{sediment}$), between horizons 1 and 2, and $t_i$ is the age of horizon $i$ deduced from an independent chronometer. $\psi$ quantifies the focusing or the winnowing between two horizons of depth $z_1$ and $z_2$ in the sediment. A value of $\psi > 1$ indicates that more $^{230}Th_{xs,0}$ has been accumulated with regard to expectation, thus indicating a lateral importation of sediment to the area, i.e., a net sediment focusing, whereas $\psi < 1$ indicates a net winnowing.

# 3 - Experimental section

## 3.1 - Sediment samples

Four cores located along the Equator have been analyzed in this study (see figure 1 for cores location). MD97-2138, referred hereafter to as MD 2138, was collected using the CALYPSO Kullemberg giant piston corer aboard the R/V Marion Dufresne during campaign IMAGE III. MD 2138 is located near the Manus Island, 300 km north of New Guinea, in the western part of the Western Pacific Warm Pool (WPWP). Core from ODP leg 138 site 849, referred hereafter to as ODP 849, and core VNTR01-08PC, referred hereafter to as VNTR 8, the site survey piston core for ODP 849, are located in the eastern equatorial Pacific (EEP) at about 850 km west of the East Pacific Rise, under the equatorial Undercurrent (EUC). MW91-9 BC36, referred hereafter to as BC 36, has been collected using a box corer during R/V Mauna Wave cruise 9 on the Ontong Java plateau.

All four cores are located above the carbonate compensation depth and far from any hydrothermal sources. ODP 849, VNTR 8, and BC 36 are far from riverine sources of terrigenous material. For these three cores, particulate matter sinking through the water column is, therefore, predominantly of biogenic origin and winds are the only

significant source of terrigenous material. On the contrary, MD 2138 is located close to the island of New Guinea where large riverine discharges occur (Milliman et al., 1999).

## 3.2 - Age models and stratigraphy

To correct the $^{231}Pa_{xs}$ and the $^{230}Th_{xs}$ from the decay since the time of deposition and to be able to correlate events between cores, an age model that gives a precision of 1 to 3 kyr, i.e., much smaller than the half-life of both isotopes, is required.

For core ODP 849, we used the age model of Mix et al. (1995) based on the comparison between $\delta^{18}O$ record on benthic foraminifer *C. Wuellerstorfi* of site 849 and the SPECMAP stack (Imbrie et al., 1984). For core MD 2138, we used an age model based on measurements of $\delta^{18}O$ in planktonic foraminifer, *G. ruber*, by Beaufort et al. (2001). The record was stacked with the SPECMAP time scale (Imbrie et al., 1984). In addition, six $^{14}C$ ages (de Garidel-Thoron, CEREGE, France, personnal communication) have helped to constrain the $\delta^{18}O$ based age model. For core BC 36, we have stacked the two $\delta^{18}O$ records on planktonic foraminifer, *P. obliquiloculata* and *G. sacculifer*, from Patrick and Thunell (1997) with the SPECMAP time scale of Imbrie et al. (1984). Two bulk $^{14}C$ ages (Broecker et al., 1999) were used to confirm the age model.

## 3.3 - Analytical procedures

$(^{231}Pa/^{230}Th)_{xs,0}$ measurements were made by single collector, sector field, inductively coupled plasma mass spectrometer (SF-ICP-MS), on a Finnigan MAT Element I.

The analytical procedure is detailed elsewhere (Pichat, S., K. W. Sims, L. Ball, R. François, and S. Brown-Leger, Sector field inductively-coupled plasma mass spectrometry determination of $^{231}Pa$ and $^{230}Th$ in sediments: methodology, optimization, precautions, and corrections, in preparation, hereafter referred to as Pichat et al., in preparation) and is only described briefly here. 200-300 mg of sediment powder was

spiked with $^{233}$Pa and $^{229}$Th prior to total dissolution in a mixture of 15 ml 8 N $HNO_3$, 5 ml concentrated HF and 7 ml concentrated $HClO_4$. The solution was left overnight to achieve spike-sample equilibration and evaporated to semi-solid. Then 20 ml of 2 N HCl was added. The solution was split into two aliquots. One aliquot, referred hereafter to as $^{231}$Pa-$^{230}$Th aliquot, was used for $^{231}$Pa and $^{230}$Th separation and analyses. The other aliquot, referred hereafter to as $^{238}$U-$^{232}$Th aliquot, corresponding to approximately 2 mg of sediment was used for direct $^{238}$U and $^{232}$Th measurements by SF-ICP-MS.

In the $^{231}$Pa-$^{230}$Th aliquot, iron oxyhydroxides that adsorb Pa and Th were precipitated by raising the pH with concentrated $NH_4OH$. The precipitate was cleaned by deionised Millipore water and 2 N HCl and was finally dissolved in 9 N HCl. Then Th and Pa were separated and purified by anion exchange chromatography following a procedure modified from Fleer and Bacon (1991) and optimized by tracer experiments, described by Pichat et al. (in preparation). Measurements were made by SF-ICP-MS in low resolution mode. The overall precision was usually better than ± 0.0025 (2σ level), i.e. 5 to 20 times better than the values previously obtained by α-counting. Several duplicate analyses have confirmed the validity of the procedure by showing a reproducibility usually better than 5 % on the $(^{231}Pa/^{230}Th)_{xs,0}$ ratio. The instrumental mass fractionation was evaluated by bracketing each sample measurement by the analysis of a U standard (NBS 960) (Pichat et al., in preparation). The contributions to the signal of the instrumental background, dark noise, blanks linked to the chemical procedure, and blanks linked to spike addition were corrected according to Pichat et al. (in preparation). Initial excess activities were obtained after corrections for (1) the detrital $^{230}$Th or $^{231}$Pa contribution, estimated from the $^{232}$Th content of the sediment (e.g. Pichat et al., in preparation), (2) the post-depositional ingrowth of the $^{230}$Th or $^{231}$Pa by authigenic uranium (e.g. Pichat et al., in preparation), and (3) the decay since the time of sediment deposition estimated from the age-model of each core (e.g. Yu, 1994).

The concentrations of Al, Ba, Ca, Fe, Mg, Mn, Si, Sr and Ti were measured for 13 samples of core MD 2138. Analyses were performed by inductively coupled plasma optical emission spectrometry (ICP-OES, Jobin Yvon JY38VHR). The biogenic Si

content of the core was calculated by subtracting the contribution of the terrigenous Si to the total Si using the value of 2.89 for the Si/Al ratio for the terrigenous material.

# 4 - Results

The downcore profiles of $(^{231}Pa/^{230}Th)_{xs,0}$ are presented in figure 2 together with the $\delta^{18}O$ records of each core. Core BC 36 is only documented for the Holocene. MD 2138 and ODP 849 have been analyzed with a resolution of 2 to 4,000 years from core-top to the end of oxygen isotope stage, referred hereafter as IS, number 5, 86,000 years before present. Thus, our total record covers the last glacial/interglacial transition but also three less extreme climatic transitions, including all of isotope stages one through four.

In core BC 36, the $(^{231}Pa/^{230}Th)_{xs,0}$ values are almost equal to the production ratio predicted by the decay of uranium in the water column (production rate) and exhibit small variation during the Holocene.

For the two other cores, the $(^{231}Pa/^{230}Th)_{xs,0}$ patterns are very similar. The $(^{231}Pa/^{230}Th)_{xs,0}$ records show high amplitude variability between glacial and interglacial periods over the Equator, with systematically lower values during glacial times, marked by IS 2 and IS 4. The variations in core ODP 849 range from 0.085 to 0.122, i.e. they are smaller than the MD 2138 variability (0.073 to 0.170). In both cores, the lower values are slightly below the production rate. Both in the WPWP (MD 2138) and in the EEP (ODP 849) the values are almost always above the production rate. This pattern suggests a nearly permanent lateral input of $^{231}Pa$ in the EEP and in the WPWP. Even during glacial periods, characterised by the lower values, there is no significant net export of $^{231}Pa$ from these two regions.

# 5 - Discussion

The BC 36 pattern reflects very stable conditions over the Ontong Java plateau during the Holocene. Moreover, during this period, all the $^{231}Pa$ produced in the water

column over the Ontong-Java plateau is either totally scavenged without lateral redistribution or that import and export of Pa roughly balance each other.

The systematically lower $(^{231}Pa/^{230}Th)_{xs,0}$ ratios during glacial times both in the EEP and the WPWP suggest that the regulating mechanism for these variations is the same for the different glacial periods. A previous study in the Pacific (Lao et al., 1992b) has shown a decrease in the LGM $(^{231}Pa/^{230}Th)_{xs,0}$ ratio at ocean margins compared to the Holocene values. Our study extends the observation of Lao and co-workers over four glacial/interglacial transitions, i.e. two glacial periods, IS 2 and IS 4, and three interglacial periods, the Holocene, IS 3 and the end of IS 5.

As mentioned in section 2, several factors can cause the deep-sea sediment $(^{231}Pa/^{230}Th)_{xs,0}$ ratio to vary: change in the lateral advection, variation in the nature of the particles, change in the intensity of the boundary scavenging resulting either from variation in the flux of material over the whole ocean or from variation in the biological productivity. On the basis of their data alone, Lao and co-authors (1992b) have not been able to consider the combined effects of all these factors. Hereafter we consider the effects of each of these factors on our data as a means to isolate the dominant ones.

## 5.1 - Influence of lateral advection by deep-water masses

The $(^{231}Pa/^{230}Th)_{xs,0}$ patterns from the equatorial Pacific seem to balance the Atlantic patterns. However, the studies from the Atlantic (e.g. Yu et al., 1996) and the Southern Ocean (e.g. Walters et al., 1997) have shown that $^{231}Pa$ exported by the NADW is scavenged in the opal belt of the Southern Ocean. Therefore, variations measured in the equatorial Pacific cannot result from the export of $^{231}Pa$ along the conveyor belt. Moreover, the present day residence time of Pacific deep-water masses of 575 years (Stuiver et al., 1983) is long compared with the $^{231}Pa$ residence time ($\tau_{Pa}$ = 50-200 years). The residence time of Pacific water is unlikely to vary by a factor of more than 2.5 during glacial periods. Thus, variability in global oceanic circulation, and therefore a variation in the lateral advection of $^{231}Pa$ by deep water masses cannot account for the variations in $(^{231}Pa/^{230}Th)_{xs,0}$ in the WPWP and the EEP.

## 5.2 - Chemical composition of the sinking particles

In core MD 2138, both manganese and biogenic opal content are lower than 1 % wt. (figure 3). Given the uncertainty on the measurements, the manganese and biogenic opal content of the core can be considered as negligible. The iron content of the core varies between 1.4 and 2.8 % wt. (figure 3), which is not significant enough to change the fractionation factor (F) between $^{231}$Pa and $^{230}$Th. In addition, these variations do not correspond systematically to glacial/interglacial variations.

Therefore we can conclude that the chemical composition of the particles has not varied significantly enough in core MD 2138 to modify the fractionation factor (F) between $^{231}$Pa and $^{230}$Th through the 85,000 years covered by the study.

The lack of information on core ODP 849 does not allow us to firmly conclude about the variability of the particle chemistry of the EEP. Though it cannot be totally disregarded, variations in the chemical composition of the settling particles probably cause negligible effects in view of the low opal concentration typically found in the sediment and settling material of the regions investigated (Farrell et al., 1995).

In conclusion, the variability in the chemical composition of the settling particles is small and is therefore not likely to cause the variations in the $(^{231}Pa/^{230}Th)_{xs,0}$ ratio in the EEP and in the WPWP over the time scale of the study.

In the following sections we will discuss two hypotheses that could explain the observed $(^{231}Pa/^{230}Th)_{xs,0}$ ratio variations. In the first hypothesis, proposed by Lao et al. (1992b), the lower $(^{231}Pa/^{230}Th)_{xs,0}$ ratios during the glacial periods are explained by an enhanced flux of particles over the entire Pacific, thus allowing more *in situ* $^{231}$Pa scavenging. Consequently, less $^{231}$Pa can be laterally exported from the open ocean to the margins and the equatorial Pacific. This hypothesis is based on the record of an increase in the Al flux normalized to $^{230}Th_{xs}$ in 15 cores of the north Pacific (Lao et al., 1992a, b). The Al flux is a proxy for terrigenous flux. Lao et al. (1992b) have therefore proposed that the globally enhanced particle flux during the LGM was a consequence of either higher eolian flux or higher $CaCO_3$ accumulation rates, like in the EEP (Archer, 1991;

Rea et al., 1991a) or off the coast of California (Lyle et al., 1992), or a combination of both phenomenon.

The second hypothesis is based on the agreement between modern productivity and $(^{231}Pa/^{230}Th)_{xs,0}$ ratio measured in surperficial sediments in the Pacific (Walter et al., 1999). The $(^{231}Pa/^{230}Th)_{xs,0}$ pattern in the EEP reflects the present days nutrient supply by the equatorial upwelling. The database in the WPWP is too patchy to allow one to draw a similar conclusion, however, the presence of equatorial upwelling in the Western Pacific (Helber and Weisberg, in press) and/or the upwelling of the Mindanao Dome (Masumoto and Yamagata, 1991) (figure 1) providing nutrient rich waters, suggests that $(^{231}Pa/^{230}Th)_{xs,0}$ variations in MD 2138 and ODP 849 are likely linked to variations in productivity.

## 5.3 - Variations of particle flux over the Pacific during the last 85,000 years

### 5.3.1 - Records of terrigenous flux in the Pacific

Since no $CaCO_3$ data were available for MD 2138 and in order to be able to compare data between ODP 849 and MD 2138 we have used the $^{232}Th$ normalized flux ($RR_{232Th}$) as a proxy for the terrigenous flux, with the commonly accepted assumption that all the $^{232}Th$ buried in the sediment has a detrital origin.

Al flux normalized to $^{230}Th_{xs}$ ($RR_{Al}$) can also be used as a terrigenous flux proxy. Lao et al. (1992b) have recorded higher $RR_{Al}$ during the LGM, with an average increase of 50 %. We have only Al data in core MD 2138 for comparison. However, the terrigenous flux variations were derived from the variations in the $^{232}Th$ normalized flux ($RR_{232Th}$). The data are shown in figure 4. The $RR_{Al}$ and the $RR_{232Th}$ in the WPWP exhibit similar trends showing the adequacy of the use of both proxies to monitor terrigenous flux patterns. Terrigenous flux patterns in the EEP and the WPWP are very similar, with an increase during the two glacial periods covered by the study. In both

cores, the $RR_{232Th}$ almost doubles. However, the detrital flux, derived from the $RR_{232Th}$ values, is ten times lower in the EEP than in the WPWP, in good agreement with $CaCO_3$ dominated vertical rain rate in the EEP (figure 5). The interpretations derived from higher carbonate accumulation rates are described in section 5.4.

### 5.3.2 - Provenance of dust in the Pacific: influence on the higher glacial detrital flux record

#### 5.3.2.1 - Source of dust in the Pacific

Asia is the source of dust for the north central Pacific (Nakai et al., 1993). The direction of dust transport over this part of the Pacific is controlled by westerlies, with maximum deposition in a band located between 37° N and 40° N, extended by a tongue flowing south to the central equatorial Pacific (Merrill et al., 1989) (figure 6). The position of this narrow band has not varied over the last 30,000 years (Rea and Leinen, 1988). There is a rapid decline in the eolian flux downwind from Asia, north and south of the latitudinal band (Rea and Leinen, 1988) and downwind along the southward tongue (Merrill et al., 1989).

The source of dust for northeast Pacific is North America, in particular the Cascades mountains (figure 6), while Central or South America are the sources for the southeast Pacific (Nakai et al., 1993). The provenance of dust in the EEP seems to be South America (Rea et al., 1991b). Dust is brought from America to the east Pacific by the westwards blowing trade winds. Finally eolian flux to the South Pacific has remained very low since the Oligocene (Rea and Bloomstine, 1986).

#### 5.3.2.2 - Glacial/interglacial variations in the dust inputs over the northwest Pacific

The atmosphere was dustier during the last glacial period than at present. This assumption is based on loess records from Asia (Kukla and An, 1989) or ice core records from east Antarctica (Petit et al., 1990). However, the enhanced eolian flux seems to be mostly linked to westerlies: the higher LGM dust flux from Asia are transported by the

north Pacific westerlies, and the higher dust inputs to east Antarctica originate from Patagonia and are therefore transported by eastwards blowing winds (Basile et al., 1997).

Sorting the variations in the Al flux calculated by Lao et al. (1992b) by regions shows a greater increase of $RR_{Al}$ in the northwest Pacific (85 %) than off the California coast (30 %) or in the EEP (11.5 %). The cores which accounts for the greatest $RR_{Al}$ increase during the LGM, noticed by Lao et al. (1992b), are located under the narrow westerlies band and under the southward flowing tongue (figure 6), in agreement with Olivarez et al. (1991) deep-sea cores data showing higher Asian dust flux in the northwestern Pacific.

#### 5.3.2.3 - Glacial/interglacial variations in the dust inputs over the equatorial Pacific

The dominant winds in the EEP and the CEP are the westward blowing trade winds. Palynologic records show that the last glacial period was less arid than the Holocene in the Andes (Hooghiemstra, 1984; Betancourt et al., 2000) and therefore less dust can be exported from this region by the trade winds. Results from deep-sea cores located in the equatorial Pacific agree with the palynologic records by showing that glacial dust flux were slightly lower or equivalent to interglacial ones (Olivarez et al., 1991).

The records from our study and from Lao et al. (1992b) study show increased detrital flux during glacial periods. Our estimates are based on $^{232}Th$ or Al fluxes that record the global detrital flux and not only the eolian flux. Therefore the 11.5% $RR_{Al}$ increase recorded by Lao et al. (1992b) does not appear to be significant enough to contradict previous conclusions. The 30 % increase in the $^{232}Th$ flux recorded in ODP 849 is more significant, however the detrital flux in ODP 849 is almost negligible. Finally, the $^{232}Th$ flux increase recorded in MD 2138 during glacial periods can be explained by the increased dust inputs brought from Asia by the Monsoons.

#### 5.3.2.4 - Glacial/interglacial variations in the dust inputs over the northeast Pacific

For the three cores located off California coast in Lao et al. (1992b) study, the $RR_{Al}$ are higher during the LGM, but the increase is less pronounced in the more remote core showing that the north Pacific gyre did not necessarily receive more dust during the

LGM. The extrapolation of the higher LGM detrital flux of these three cores, located near the coast, to the north Pacific gyre is therefore likely to create a bias.

#### 5.3.2.5 - Conclusion

The glacial/interglacial variability in the patterns of dust input over the Pacific seems to be rather complex and is likely to create local effects. The hypothesis of Lao et al. (1992b) appears to be biased by the high number of cores analyzed in their study which were located under the narrow westerlies band, where most of the dust flux variability occurs between glacial and interglacial periods (figure 6).

### 5.3.3 - Total flux variability in the WPWP and the EEP

The total flux normalized to $^{230}Th_{xs}$ (Eq. 1) in the EEP and the WPWP do show either no variation or a slight decrease during glacial times (figure 7). Hence, it contradicts Lao et al. (1992b) hypothesis of higher flux over the whole Pacific.

## 5.4 - Productivity variations in the EEP and the WPWP over the last 85,000 years

Hypothesizing that the $(^{231}Pa/^{230}Th)_{xs,0}$ ratio records export productivity variations in the WPWP and in the EEP implies a systematically lower productivity during MIS 2 and the less extreme MIS 4, i.e. the colder periods over the last 85,000 years. This challenges the commonly accepted behavior that productivity was higher during glacial times. Evidence for higher productivity in the glacial equatorial Pacific comes from increased accumulation rates of calcium carbonate (Lyle et al., 1988; Rea et al., 1991a; Archer, 1991), organic carbon (Pedersen, 1983; Lyle et al., 1988; Sarthein et al., 1988), Al excess (Murray and Leinen, 1996, Murray et al., 1993), and barite (Paytan et al., 1996) during glacial periods. However, all these proxies of productivity are

sensitive to both carbonate dissolution and sediment redistribution after deposition, i.e., focusing or winnowing.

### 5.4.1 - Sediment redistribution by deep currents

To test sediment redistribution in the EEP, we have measured ($^{230}Th_{xs,0}$) in core VNTR 8 because $CaCO_3$ and $BaSO_4$ accumulation rates were available for this core. In both ODP 849 and VNTR 8, the focusing factors, derived from Eq. 3, are higher than 1 showing a permanent focusing at the Equator. Our observations confirm results from Higgins et al. (1999) showing that sediments accumulate more rapidly on-equator than a few degrees of latitude off-equator. Enhanced focusing occurs during IS 2 and IS 4 (figure 8) and therefore could artificially increase the accumulation rates derived from $\delta^{18}O$ values of each individual component of the sediment. This phenomenon could explain the discrepancy between our conclusions and the conclusions derived from other proxies, which are sensitive to sediment remobilization. We have compared the $\delta^{18}O$-derived accumulation rates, referred hereafter as AR, with the $^{230}Th_{xs,0}$ normalized flux ($RR_i$, calculated with Eq. 2) of barite and calcium carbonate, in core VNTR 8. Results are shown in figure 9. Normalization to $^{230}Th_{xs,0}$ of both barite and carbonate contents eliminates most of the variability observed in the $\delta^{18}O$-derived accumulation rates. In particular, the increase observed in both the BaAR and the $CaCO_3$AR during the last glacial period turns out to be insignificant after normalization to $^{230}Th_{xs,0}$ ($RR_{Ba}$ and $RR_{CaCO3}$). These observations are similar to the recent observation by Marcantonio and co-workers (2001) in the CEP on core TT013-PC72 (0°06.8' N 139°24.1' W) showing that higher BaAR occurs during higher sediment focusing. They have also shown that the normalization to $^{230}Th_{xs,0}$ of the Ba content in TT013-PC72, analyzed by Paytan et al. (1996), eliminates most of the BaAR variability. Therefore, on this basis, the conclusion of Paytan et al. (1996) of higher glacial productivity, in both the EEP and the CEP, deduced from $\delta^{18}O$-derived barite accumulation rates can be ruled out. Higher glacial $\delta^{18}O$-derived accumulation rates turn to be linked to enhanced sediment focusing rather than to enhanced productivity. Thus, the higher glacial productivity derived from organic carbon, carbonate, Ba, or $Al_{xs}$ accumulation rates can be questioned.

### 5.4.2 - Other proxies supporting lower biological productivity during glacial periods

The hypothesis of lower biological productivity during glacial periods in the EEP and the WPWP is supported by recent studies in the EEP (Loubere, 2000), based on a benthic foraminifer transfer function, and in the WPWP (Beaufort et al., 2001), based on the abundance of *F. profunda* in a coccolithofores assemblage (Beaufort et al., 1997). These studies have demonstrated a glacial decrease in the productivity. In both studies, a test has been performed to demonstrate the insensitivity of the proxies to dissolution.

Finally, the $(^{231}Pa/^{230}Th)_{xs,0}$ ratios in three cores of the CEP, at 140° W, exhibit an increase from the LGM to the Holocene (Stephens and Kadko, 1997), in agreement with our EEP and WPWP records.

### 5.4.3 - Effect of the $CaCO_3$ dissolution in the water column

The calcium carbonate rain rates are probably higher than measured because of the effect of dissolution in the water column. Studies in the CEP (Stephens and Kadko, 1997) and in the EEP (Le et al., 1995) have concluded that higher dissolution of $CaCO_3$ has occurred during interglacial periods. Applying a dissolution correction would therefore increase the interglacial $CaCO_3$ accumulation rates more than the glacial ones. Considering the effect of sediment focusing (figure 9a) the dissolution correction would result in showing that $CaCO_3$ accumulation rates were higher during interglacial periods and therefore that the biological productivity was higher during interglacial periods. Although it has to be quantified, the effect of dissolution combined with sediment focusing reconciles the conclusions on glacial/interglacial biological productivity variations derived from $(^{231}Pa/^{230}Th)_{xs,0}$ ratios and $CaCO_3$ accumulation rates.

### 5.4.4 - Consequence on Lao et al. (1992b) hypothesis

One of the hypothesis proposed by Lao et al. (1992b) to explain enhanced glacial particle flux over the whole Pacific was higher $CaCO_3$ flux in some regions, in

particular the EEP. In the light of our data, it appears that glacial $CaCO_3$ accumulation rates were equivalent or even slightly lower than interglacial ones, along the equator, thus weakening Lao et al. (1992b) hypothesis.

### 5.4.5 - Conclusions

Distinguishing between higher detrital glacial flux and lower glacial productivity hypothesis appears rather complex. The record of higher detrital flux MD 2138 and ODP 849 during IS 2 and to a lesser extent during IS 4 tends to support the hypothesis proposed by Lao et al. (1992b), however detrital flux patterns have a strong local signature reflecting the various sources of dust of the Pacific Ocean. Lao et al. (1992b) study could have been biased by these local effects. During the glacial periods $CaCO_3$ accumulation rates were artificially increased compared to interglacial periods by sediment focusing and possibly by dissolution effects. Therefore, we prefer to attribute the systematically lower $(^{231}Pa/^{230}Th)_{xs,0}$ ratio recorded in ODP 849 and MD 2138 during glacial periods to a decrease in productivity. This hypothesis is supported by similar conclusions derived either from the same proxy in cores of the CEP (Kadko and Stephens, 1997) or from fossils assemblage proxies in cores from the EEP (Loubere, 1999; 2000) and the WPWP (Beaufort et al., 2001), which have been tested for their insensitivity to dissolution. Furthermore, the apparent discrepancy between our data and the conclusions derived from carbonate or barite accumulation rates vanished when sediment focusing is considered by using $^{230}Th_{xs,0}$ normalized flux instead of $\delta^{18}O$-derived accumulation rates, in spite of a potential bias linked to the lack of constraints on the spatial extension of the sediment focusing,

## 5.5 - Potential cause of lower glacial productivity in the EEP and in the WPWP and compatibility with observations deduced from other proxies

The data of Lao et al. (1992b) show that part of the northwest Pacific $(^{231}Pa/^{230}Th)_{xs,0}$ ratio variability can arise from variations in the Asian dust inputs.

However, in the EEP and in the WPWP the $(^{231}Pa/^{230}Th)_{xs,0}$ ratio variability appears to be associated with lower glacial productivity.

Productivity can decrease in response to two main processes: (1) limitation in the major nutrient supply to the euphotic zone caused by a decline in the intensity of upwellings, by an increase in the vertical stratification of the ocean, or by a change in the nutrient concentration in the major currents or (2) limitation in the efficiency of the use of major nutrients by limiting micronutrients, like iron, or a shift in the plankton community.

### 5.5.1 - Limitation in the major nutrient supply to the euphotic zone

During the LGM, sea surface temperatures in the EEP were lower than during the Holocene showing higher upwelling rates (Lyle et al., 1992). This intensification of the equatorial upwelling is confirmed by pH reconstructions based on boron isotopes (Sanyal et al., 1997). The intensification of upwelling would increase the nutrient content of the euphotic zone and thereby the productivity, which apparently contradicts our observations.

There was a decrease in the nitrate utilization north of the Modern Polar Front during the LGM as shown by the decrease of the $\delta^{15}N$ (François et al., 1997). The Peru current originating in these regions will therefore have a higher nitrate content and a lower $\delta^{15}N$. In addition, the equatorial upwelling originate the shallow waters of the EUC (Tomzack and Bradley, 1994) and in the EEP, the EUC is entrained to the surface between 110° W and 95°W. Since the lower layers of the EUC originates in the subantarctic region of the southwest Pacific where Subantarctic Mode Water is formed (Toggweiler et al., 1991) and the Peru currents feeds the SEC and the EEP (figure 1), the equatorial upwelling and the EEP are likely to be enriched in nitrate during the last glacial periods.

A $\delta^{15}N$ decrease has been observed in three cores of the EEP, between 84 and 91°W, during the LGM (Farell et al., 1995). It has been interpreted as reflecting a supply of nitrate to the surface ocean by upwelling greater than the uptake by plankton. It is

consistent to reinterpret these data as reflecting a lower nutrient utilization and correlatively lower productivity. Lower nutrient utilization in spite of a higher nitrate content of upwelled waters and inputs of nitrate from the Peru current points out a limiting factor to cause the low productivity. Iron is the most likely to have this role (Martin and Fitzwater, 1988).

### 5.5.2 - Limitation in the efficiency of the use of nutrients

Dust fluxes to the EEP have not varied significantly between the glacial and the interglacial periods (Olivarez, 1991 and our study). Therefore increased iron limitation during glacial periods cannot arise from eolian inputs. A potential important source of iron to the sea comes from continental weathering. One of the greatest loads of continental sediments to the ocean takes place north of the island of New Guinea (860 t $y^{-1}$, Milliman et al., 1999). The continental discharge north of New Guinea is made on a narrow shelf which is easily by passed (Milliman et al., 1999). In addition most of the rivers have small or non-existent estuaries (Milliman et al., 1999). Continental inputs are consequently transported directly to the slope and off the coast. The island weathering Rare Earth Elements (REE) signature is propagated to the EUC (Sholkovitz et al., 1999) showing that New Guinea riverine inputs feeds the EUC. During glacial periods the sea level in this area has lowered by 100-120 meters (Bard et al., 1990; Bard et al., 1996; Lambeck and Chappell, 2001). The extension of the shelf was therefore greater, and riverine inputs started to accumulate on the shelf, notably those coming from the Sepik River, the main river flowing to the north coast of New Guinea (Milliman et al., 1999). Fe, REE, and humic acids are present in a colloid phase in rivers (Elderfield et al., 1990). Removal of REE has been observed in most of the estuaries because of a salt-induced coagulation of the colloids (Elderfield et al., 1990; Sholkovitz et al., 1993; 1995). A similar pattern is likely to occur for iron. The extension of the shelf increased the size of estuaries allowing more Fe to be removed during the glacial periods. All these elements tend to show that less Fe was exported into the EUC during glacial periods and that consequently less Fe was upwelled in the equatorial Pacific. Since the WPWP is

connected to New Guinea but also to the EUC via the NEC (figure 1), a similar decrease of Fe inputs is likely to occur during glacial periods.

Altabet (2001) has shown that the relative utilization of $NO_3^-$ (u) is controlled by the product of the $Fe/NO_3^-$ ratio delivery by upwelling and the $NO_3^-/Fe$ ratio of utilization by plankton (Eq. 4):

$$u = \left(\frac{[Fe]}{[NO_3^-]}\right)_{upwelled} \times \left(\frac{NO_3^-}{Fe}\right)_{utilized} \quad (4)$$

Altabet argued that $(NO_3^-/Fe)_{utilized}$ has remained constant through the last 600 kyr. Since there is an increase of the $NO_3^-$ concentration and a decrease of the Fe concentration in the upwelled waters at the Equator during glacial periods the relative utilization of $NO_3^-$ is decreased. This pattern explains the lower $\delta^{15}N$ observed by Farrell et al. (1995) during the LGM. Additionally, the lower Fe content of the upwelled waters limits more severely the biological productivity during IS2 and IS4. This conclusion is also in good agreement with higher $CO_2$ efflux from the EEP to the atmosphere during glacial periods, as the intensification of the equatorial upwelling brought more $CO_2$ to the surface ocean and the decrease in productivity reduced the $CO_2$ transfer to the deep ocean by biological pumping. Verifying these hypotheses would require a better data coverage of the Pacific. This higher transfer of $CO_2$ from the equatorial Pacific to the atmosphere during glacial periods has to be taken into account in the models of global atmospheric drawdown.

The hypotheses of a shift in the plankton community or of silica limitation (Leynaert et al., 2001) cannot be fully evaluated with the available data.

# 6 - Conclusions

We have shown that the $(^{231}Pa/^{230}Th)_{xs,0}$ values in the EEP and in the WPWP are systematically lower during glacial periods over the last 86,000 years. The hypothesis that the $(^{231}Pa/^{230}Th)_{xs,0}$ ratio is controlled by the variability in dust supply to the Pacific proposed by Lao et al. (1992b) cannot be definitively ruled out. However, given the multiple dust sources of the Pacific Ocean, the wind path over the Pacific, and the

difference in the behavior of the source of dust in response to glacial/interglacial changes it is likely that variations controlled by dust input only would create local patterns rather than the systematic $(^{231}Pa/^{230}Th)_{xs,0}$ ratio distribution observed in the Pacific. Rather the $(^{231}Pa/^{230}Th)_{xs,0}$ ratio can be used as a productivity proxy in the EEP and in the WPWP. Therefore the $(^{231}Pa/^{230}Th)_{xs,0}$ data indicates a lower productivity during glacial periods. The cause of the productivity decrease could arise from lower continental inputs from New Guinea which would lower the concentration of iron in the EUC and correlatively in the equatorial upwelling. Confirming this hypothesis requires further investigations, in particular an extension of the $(^{231}Pa/^{230}Th)_{xs,0}$ database in the Pacific. Nevertheless, the lower glacial productivity in the EEP and in the WPWP inferred from $(^{231}Pa/^{230}Th)_{xs,0}$ measurements is in good agreement with the lower glacial utilization of nitrate in the EEP derived from $\delta^{15}N$ measurements, and the intensification of the equatorial upwelling. Lower glacial productivity would intensify the transfer of $CO_2$ from the ocean to the atmosphere in the Pacific Ocean as a result of the lower biological pumping combined with the intensification of the equatorial upwelling.

Finally, the conclusions of high sediment focusing in the EEP corroborate the results by Marcantonio et al. (2001). Enhanced glacial sediment focusing causes an apparently higher $\delta^{18}O$-derived sediment accumulation rate during glacial periods. The influence of sediment focusing has been proven to be great on the carbonate and the barite excess accumulation rates. The correction of the effect of the sediment focusing leads to a reinterpretation of the $\delta^{18}O$-derived accumulation rate data. The higher glacial carbonate and barite $\delta^{18}O$-derived accumulation rates vary insignificantly variations when normalized to $^{230}Th_{xs,0}$. Accordingly, we suggest using $^{230}Th_{xs,0}$ normalized fluxes instead of the $\delta^{18}O$-derived accumulation rates.

**Acknowledgements**: We thank L. Ball and the WHOI ICP Facility for use of the Finnigan MAT Element I sector field inductively coupled plasma mass spectrometer (SF-ICP-MS) and theJobin Yvon JY38VHR ICP-OES. We thank S. J. Manganini for performing analyses of oxides. S. P. gratefully acknowledges the support of the CNRS-NSF, the Eurodoc program of the Région Rhône-Alpes, and the Geology and Geophysics Dept (WHOI). S. P. is also grateful to S. Brown-Leger and A. P. Fleer for their help in the laboratory.

## References

Altabet, M. A., Nitrogen isotopic evidence for micronutrient control of fractional $NO_3^-$ utilization in the Equatorial Pacific: *Limnol. Oceanogr*. **46**, 368-380, 2001.

Anderson, H. L., R. François, and S. B. Moran, Experimental evidence for differential adsorbtion of Th and Pa on different solid phases in seawater, *EOS, Trans. Amer. Geophys. Union* **73**, 270, 1992.

Anderson, R. F., M. P. Bacon, and P. G. Brewer, Removal of $^{230}$Th and $^{231}$Pa from the open ocean, *Earth Planet. Sci. Lett.* **62**, 7-23, 1983a.

Anderson, R. F., M. P. Bacon, and P. G. Brewer, Removal of $^{230}$Th and $^{231}$Pa from the ocean margins, *Earth Planet. Sci. Lett.* **66**, 73-90, 1983b.

Archer, D. E., Equatorial Pacific calcite preservation cycles: production or dissolution ?, *Paleoceanography* **6**, 561-571, 1991.

Bacon, M. P., Tracers of chemical scavenging in the ocean: boundary effects and large-scale chemical fractionation, *Philos. Trans. R. Soc. London, Ser. A* **325**, 147–160, 1988.

Bacon, M. P., Glacial to interglacial changes in carbonate and clay sedimentation in the Atlantic Ocean estimated from $^{230}$Th measurements, *Isot. Geosci.* **2**, 97-111, 1984.

Bacon, M. P., and J. N. Rosholt, Accumulation rates of $^{230}$Th, $^{231}$Pa, and some transition metals on the Bermuda Rise, *Geochim. Cosmochim. Acta* **46**, 651-666, 1982.

Bard, E., B. Hamelin, M. Arnold, L. Montaggioni, G. Cabioch, G. Faure, and F. Rougerie, Deglacial sea-level record from Tahiti corals and the timing of global meltwater discharge, *Nature* **382**, 241-244, 1996.

Bard, E., B. Hamelin, and R. G. Fairbanks, U-Th ages obtained by mass spectrometry in corals from Barbados: Sea level during the past 130,000 years, *Nature* **346**, 456-458, 1990.

Barnola, J. M., D. Raynaud, Y. S. Korotkevich, and C. Lorius, Vostock ice core provides 160,000-year record of atmospheric $CO_2$, *Nature* **329**, 408-413, 1987.

Basile, I., F. E. Grousset, M. Revel, J. R. Petit, P. E. Biscaye, and N. I. Barkov, Patagonian origin of glacial dust deposited in East Antarctica (Vostok, Dome C) during glacial stages 2, 4, and 6, *Earth Planet. Sci. Lett.* **146**, 573-589, 1997.

Beaufort, L., T. de Garidel-Thoron, A. C. Mix, and N. G. Pisias, ENSO-like forcing on oceanic primary production during the late Pleistocene, *Science* **293**, 2440-2444, 2001.

Beaufort, L., Y. Lancelot, P. Camberlin, O. Cayre, E. Vincent, F. Bassinot, L. Labeyrie, Insolation cycles as a major control of Equatorial Indian ocean primary production, *Science* **278**, 1451-1454, 1997.

Berger, W. H., V. Smetacek, and G. Wefer,. Ocean productivity and paleoproductivity - An overview. In *Productivity of the Ocean: Present and Past*, Berger, W. H., V. Smetacek, V., and G. Wefer (Eds), Dahlem Workshop Reports, John Wiley & Sons, Chichester, 1-34, 1989.

Berger, W. H., K. Fisher, C. Lai, and G. Wu, Ocean carbon flux: global maps of primary production and export production. In *Biogeochemical cycling and fluxes between the deep euphotic zone and other oceanic realms*, Agegian, C. R. (Ed) NOAA National Undersea Research Program, Res. Rpt. 88-1, 1988.

Betancourt, J. L., C. Latorre, J. A. Rech, J. Quade, K. A. Rylander, A 22,000-year record of monsoonal precipitation from northern Chile's Atacama desert, *Science* **289**, 1542-1546, 2000.

Betzer, P. R., W. J. Showers, E. A. Laws, C. D. Winn, G. R. DiTullio, and P. M. Kroopnick, Primary production and particle fluxes on a transect of the equator at 153° W in the Pacific Ocean, *Deep Sea Res.* **31**, 1-11, 1984.

Boutin, J., and J. Etcheto, Long-term variability of the air-sea $CO_2$ exchange coefficient: Consequences for the $CO_2$ fluxes in the equatorial Pacific Ocean, *Global Biogeochem. Cycles* **11**, 453-470, 1997.

Brewer, P. G., Y. Nozaki, D. W. Spencer, and A. P. Fleer, Sediment trap experiments in the deep North Atlantic: isotopic and elemental fluxes, *J. Marine Research* **38**, 703-728, 1980.

Brewer, P.G., Minor elements in seawater. In *Chemical Oceanography*, Vol. 1, 2nd Edition, Riley, J. P., and G. Skirrow (Eds), Academic Press, New York, U.S.A.,415-496, 1975.

Broecker, W. S., E. Clark, D. C. McCorkle, I. Hajdas, and G. Bonani, Core top $^{14}C$ ages as a function of latitude and water depth on the Ontong-Java plateau, *Paleoceanography* **14**, 13-22, 1999.

Broecker, W. S., and T.-H. Peng, *Tracers in the Sea*, Eldigio Press, Lamont-Doherty Geological Observatory of Columbia University, Palisades, New York, 690 pp, 1982.

Cane, M. A., A role for the tropical Pacific, *Science* **282**, 59-61, 1998.

Clement, A. C., R. Seager, and M. A. Cane, Orbital controls on the El Niño/Southern Oscillation and the tropical climate, *Paleoceanography* **14**, 441-456, 1999.

Chen, J. H., R. L. Edwards, and G. J. Wasserburg, $^{238}$U-$^{234}$U-$^{232}$Th in seawater, *Earth Planet. Sci. Lett.* **80**, 241-251, 1986.

Dandonneau, Y, Sea-surface partial-pressure of carbon-dioxide in the eastern equatorial Pacific (August 1991 to October 1992): A multivariate analysis of physical and biological factors, *Deep Sea Res. B* **42,** 349-364, 1995.

Dehairs, F., R. Chesselet, and J. Jedwab, Discrete suspended particles of barite and the barium cycle in the open ocean, *Earth Planet. Sci. Lett.* **49**, 528-550, 1980.

Deuser, W. G., E. H. Ross, and R. F. Anderson, Seasonality in the supply of sediment to the deep Sargasso Sea and implications for the rapid transfer of matter to the deep ocean, *Deep-Sea Res. A* **28**, 495-505, 1981.

Elderfield, H., R. Upstill-Goddard, and E. R. Sholkovitz, The rare earth elements in rivers, estuaries and coastal sea waters: processes affecting crustal input of elements to the ocean and their significance to the composition of sea water, *Geochim. Cosmochim. Acta* **54**, 971-991, 1990.

Emerson, S., P. Quay, D. Karl, C. Winn, L. Tupas, and M. Landry, Experimental Determination of the Organic Carbon Flux from Open-Ocean Surface Waters, *Nature* **389,** 951-954, 1997.

Farrell J. W., I. Raffi, T. R. Janecek, D. W. Murray, M. Levitan, K. A. Dadey, K.-C.Emeis, M. Lyle, J.-A. Flores, and S. Hovan, Late Neogene sedimentation patterns in the eastern equatorial Pacific Ocean. In *Proc. ODP, Sci. Results, 138*, Pisias, N. G., L. A. Mayer, T. R. Janecek, A. Palmer-Julson, and T. H. van Andel (Eds), College Station, TX (Ocean Drilling Program), U.S.A., 717-756, 1995.

Firestone, R. B., *Table of isotopes*, 8$^{th}$ Edition, Shirley, V. S. (Ed), John Wiley & Sons, New York, U.S.A., 1996.

Fleer, A.P., and M. P. Bacon, Notes on some techniques of marine particle analysis used at WHOI. In *Marine Particles: Analysis and Characterization*, Hurd, D. C., and D. W. Spencer (Eds), *Geophys. Monograph.* **63**, AGU, 223-226, 1991.

Frank, M., R. Gersonde, and A. Mangini, Sediment redistribution, $^{230}Th_{ex}$ - normalization and implications for the reconstruction of particle flux and export paleoproductivity. In *Use of proxies in paleoceanography: Examples from the South Atlantic*, Fischer, G., and G. Wefer (Eds), Springer-Verlag, Berlin Heidelberg, Germany, 410-426, 1999.

Frank, M., J.-D. Eckhardt, A. Eisenhauer, P. W. Kubik, B. Dittrich-Hannen, M. Segl, and A. Mangini, Beryllium 10, Thorium 230, and Protactinium 231 in Galapagos microplate sediments: implications of hydrothermal activity and paleoproductivity changes during the last 100,000 years, *Paleoceanography* **9**, 559-578, 1994.

François, R. F., M. A. Altabet, E.-F. Yu, D. M. Sigman, M. P. Bacon, M. Frank, G. Bohrmann, G. Bareille, and L. D. Labeyrie, Water column stratification in the Southern Ocean contributed to the lowering of glacial atmospheric $CO_2$, *Nature* **389**, 929-935, 1997.

François, R., M. P. Bacon, M. A. Altabet, and L. D. Labeyrie, Glacial/interglacial changes in sediment rain rate in the Indian sector of Subantarctic water as recorded by $^{230}Th$, $^{231}Pa$, U, and $^{15}N$, *Paleoceanography* **8**, 611-629, 1993.

François, R., Bacon, M. P. and D. O. Suman, Thorium-230 profiling in deep-sea sediments: High-resolution records of flux and dissolution of carbonate in the equatorial Atlantic during the last 24,000 years, *Paleoceanography* **5**, 761-787, 1990.

Helber, R. W., and R. H. Weisberg, Equatorial upwelling in the western Pacific warm pool, *J. Geophysical Res.*, in press.

Henderson, G. M., C. Heinze, R. F. Anderson, and A. M. E. Winguth, Global distribution of the $^{230}Th$ flux to ocean sediments constrained by GCM modeling, *Deep-Sea Res.* **46**, 1861-1893, 1999.

Higgins, S. M., W. S. Broecker, R. F. Anderson, D. C. McCorkle, and D. Timothy, Enhanced sedimentation along the Equator in the Western Pacific, *Geophys. Res. Lett.* **26**, 3489-3492, 1999.

Holmen, K. J., The global carbon cycle. In *Global Biogeochemical Cycles*, Butcher, S. S., R. J. Charlson, G. H. Orians, and G. V. Wolfe (Eds), Academic Press, London, U. K., 239-262, 1992.

Hooghiemstra, H., Vegetational and climatic history of the high plain of Bogota, Colombia: A continuous record of the last 3.5 million years, *Dissertationes Botanicae*, Cramer, Vaduz, Liechtenstein, 1984.

Huh, C.-A., and T. M. Beasley, Profiles of dissolved and particulate thorium isotopes in the water column of coastal Southern California, *Earth Planet. Sci. Lett.* **85**, 1-10, 1987.

Imbrie, J., J. D. Hays, D. G. Martinson, A. McIntyre, A. C. Mix, J. J. Morley, N. G. Pisias, W. L. Prell, and N. J. Shackleton, The orbital theory of Pleistocene climate: Support from a revised chronology of the marine $\delta^{18}O$ Record. In *Milankovitch and Climate*, Part 1, Berger, A. L. et al. (Eds), 269-235, Hingham, MA, U.S.A., 1984.

Isern, A. R., Calcium carbonate and organic carbon accumulation in the Central Equatorial Pacific, M.S. thesis, Grad. Sch. Oceanogr., Univ. R.I., Narragansett, RI, U.S.A., 197 pp, 1991.

Kadko, D., a detailed study of some uranium series nuclides at an abyssal hill area near the East Pacific Rise at 8°45'N, *Earth Planet. Sci. Lett.* **51**, 115-131, 1980.

Ku, T.-L., K. G. Knauss, and G. G. Matthieu, Uranium in open ocean: Concentration and isotopic composition, *Deep Sea Res.* **24**, 1002-1017, 1977.

Kukla, G., and Z. An, Loess stratigraphy in central China, *Paleogeogr. Paleoclim. Paleoecol.* **72**, 203-225, 1989.

Kumar, N., R. F. Anderson, R. A. Mortlock, P. N. Froelich, P. Kubik, B. Dittrich-Hannen, and M. Suter, Increased biological productivity and export production in the glacial Southern Ocean, *Nature* **378**, 675-680, 1995.

Kumar, N., G. Gwiazda, R. F. Anderson, and P. N. Froelich, $^{231}Pa/^{230}Th$ ratios in sediments as a proxy for past changes in the Southern Ocean productivity, *Nature* **362**, 45-48, 1993.

Lambeck, K., and J. Chappell, Sea level change through the last glacial cycle, *Science* **292**, 679-686, 2001.

Lange, C. B., and W. H. Berger, Diatom productivity and the preservation in the Western Pacific: the Quaternary record. In Berger W.H. et al. (Eds), Proc. ODP, Sci. Results 130, College Station, TX, U.S.A., 509-523, 1993.

Lao, Y., R. F. Anderson, W. S. Broecker, H.-J. Hofmann, and W. Wolfli, Particulate fluxes of $^{230}Th$, $^{231}Pa$, and $^{10}Be$ in the northeastern Pacific Ocean, *Geochim. Cosmochim. Acta* **57**, 205-217, 1992a.

Lao, Y., R. F. Anderson, and W. S. Broecker, Boundary scavenging and deep-sea sediment dating: constraints from excess $^{230}$Th and $^{231}$Pa, *Paleoceanography* **7**, 783-798, 1992b.

Lao, Y., Transport and burial rates of $^{10}$Be and $^{231}$Pa in the Pacific Ocean, Ph.D. thesis, Columbia Univ., NY, 1991.

Laynaert, A., P. Tréguer, C. Lancelot, and M. Rodier, Silicon limitation of biogenic silica production in the Equatorial Pacific, *Deep Sea Res. A* **48**, 639-660, 2001.

Le J., A. C. Mix, and N. J. Shackleton, Late Quaternary paleoceanography in the eastern equatorial Pacific Ocean from planktonic foraminifers: A high-resolution record from site 846. In *Proc. ODP, Sci. Results, 138*, Pisias, N. G., L. A. Mayer, T. R. Janecek, A. Palmer-Julson, and T. H. van Andel (Eds), College Station, TX (Ocean Drilling Program), U.S.A., 675-693, 1995.

Lea, D. W., D. K. Pak, and H. J. Spero, Climate impact of late Quaternary equatorial Pacific sea surface temperature variations, *Science* **289**, 1719-1724, 2000.

Loubere, P., Marine control of biological production in the eastern equatorial Pacific Ocean, *Nature* 406, 497-500, 2000.

Loubere, P., A multiproxy reconstruction of biological productivity and oceanography in the eastern equatorial Pacific for the past 30,000 years, *Marine Micropal.* **37**, 173-198, 1999.

Lyle, M. W., F. G. Prahl, and M. A. Sparrow, Upwelling and productivity changes inferred from a temperature record in the central equatorial Pacific, *Nature* **355**, 812-815, 1992.

Lyle, M., D. W. Murray, B. P. Finney, J. Dymond, J. M. Robbins, and K. Brooksforce, The record of the late Pleistocene biogenic sedimentation of the eastern tropical Pacific Ocean, Paleoceoceanography **3**, 39-59, 1988.

Marcantonio F., R. F. Anderson, S. Higgins, M. Stute, and P. Schloesser, Sediment focusing in the central equatorial Pacific Ocean, *Paleoceanography* **16**, 260-267, 2001.

Martin, J. H., Glacial-interglacial $CO_2$ change: the iron hypothesis, *Paleoceanography* **5**, 1-13, 1990.

Martin, J. H., and Fitzwater S. E., Iron deficiency limits phytoplankton growth in the north-east Pacific subarctic, *Nature* **331,** 341-343, 1988.

Masumoto, Y., and T. Yamagata, Response of the western tropical Pacific to the Asian winter monsoon: the generation of the Mindanao Dome, *J. Phys. Ocean.* **21**, 1386-1398, 1991.

McElroy, M. B., Marine biological productivity controls on atmospheric $CO_2$ and climate, *Nature* **302**, 328-329, 1983.

Merill, J. T., M. Uematsu, and R. Bleck, Meteorological analysis of long range transport of mineral aerosols over the North Pacific, *J. Geophys. Res.* **94**, 8554-8598, 1989.

Milliman, J. D., K. L. Farnsworth, and C. S. Albertin, Flux and fate of fluvial sediments leaving large islands in the East Indies, *J. Sea Res.* **41**, 97-107, 1999.

Mix, A. C., N. G. Pisias, W. Rugh, J. Wilson, A. Morey, and T. K. Hagelberg, Benthic foraminifer stable isotope record from site 849 (0-5 Ma): local and global climate changes. In *Proc. ODP, Sci. Results, 138,* Pisias, N. G., L. A. Mayer, T. R. Janecek, A. Palmer-Julson, and T. H. van Andel (Eds), College Station, TX (Ocean Drilling Program), U.S.A., 371-412, 1995.

Müller, P. J., and E. Suess, Productivity, sedimentation rate, and organic matter in the oceans I: Organic carbon preservation, *Deep Sea Res.* **26**, 1347-1362, 1979.

Murray, R.W., and M. Leinen, Scavenged excess Al and its relationship to bulk Ti in biogenic sediment from the central equatorial Pacific ocean, *Geochim. Cosmochim. Acta* **60**, 3869-3878, 1996.

Murray, R. W., M. Leinen, and A. R. Isern, Biogenic flux of Al to sediment in the central Equatorial Pacific Ocean: Evidence for increased productivity during glacial periods, *Paleoceanography* **8**, 651-671, 1993.

Nakai, S., A. N. Halliday, and D. K. Rea, Provenance of dust in the Pacific Ocean, *Earth Planet. Sci. Lett.* **119**, 143-157, 1993.

Neftel ,A., H. Oeschger, J. Schwander, B. Stauffer, and R. Zumbrunn, Ice core measurements give atmospheric $CO_2$ content during the past 40,000 yr, *Nature* **295**, 220-223, 1982.

Nelson, D. M., P. Treguer, M. A. Brzenzinski, A. Leynaert, B. Quequinner, Production and dissolution of biogenic silica in the ocean: Revised global estimates, comparison with regional data and relationship to biogenic sedimentation, *Global Biogeochem. Cycles* **9**, 359-372, 1995.

Nozaki, Y., and T. Nakanishi, $^{231}$Pa and $^{230}$Th profiles in the open ocean water column, *Deep Sea Res.* **32**, 1209-1220, 1985.

Nozaki, Y., Y. Horibe, and H. Tsubota, The water column distributions of thorium isotopes in the western North Pacific, *Earth Planet. Sci. Lett.* **54**, 203-216, 1981.

Olivarez, A. M., R. M. Owen, and D. K. Rea, Geochemistry of eolian dust in Pacific pelagic sediments: Implications for paleoclimactic interpretations, *Geochim. Cosmochim. Acta* **55**, 2147-2158, 1991.

Patrick, A., and R. C. Thunell, Tropical Pacific sea surface temperature and upper water column thermal structure during the last glacial maximum, *Paleoceanography* **12**, 649-657, 1997.

Paytan, A., M. Kastner, and F. Chavez, Glacial to interglacial fluctuations in productivity in the equatorial Pacific as indicated by marine barite, *Science* **274**, 1355-1357, 1996.

Pedersen, T. F., Increased productivity in the eastern equatorial Pacific during the last glacial maximum (19,000 to 14,000 yr B.P.), *Geology* **11**, 16-19, 1983.

Petit, J. R., L. Mounier, J. Jouel, Y. S. Korotkevich, V. I. Kotlyakov, and C. Lorius, Paleoclimatological and chronological implications of the Vostok core dust record, *Nature* **343**, 56-58, 1990.

Rea, D. K., Hovan S.A., and T. R. Janecek, Late Quaternary flux of eolian dust to the pelagic ocean. In *Global sedimentary Geofluxes*, Hays, W.W. (Ed), N$^{al}$ Academy of Science, National Research council, 116-124, 1991b.

Rea, D. K., N. G. Pisias, and T. Newberry, Late Pleistocene paleoclimatology of the central equatorial Pacific: Flux patterns of biogenic sediments, *Paleoceanography* **6**, 227-244, 1991a.

Rea, D. K., and M. Leinen, Asian aridity and the zonal westerlies: Late Pleistocene and Holocene record of eolian deposition in the northwest Pacific Ocean, *Paleogeogr. Paleoclim. Paleoecol.* **66**, 1-8, 1988.

Rea, D. K., and M. K. Bloomstine, Neogene history of the south Pacific tradewinds: Evidence of hemispherical asymmetry of atmospheric circulation, *Paleogeogr. Paleoclim. Paleoecol.* **55**, 55-64, 1986.

Sanyal, A., N. G. Hemming, W. S. Broecker, and G. N. Hanson, Changes in pH in the Eastern Equatorial Pacific across stage 5-6 boundary based on boron isotopes in foraminifera, *Global Biogeochem. Cycles* **11**, 125-133, 1997.

Sarthein, M., K. Winn, J.-C. Duplessy, and M. R. Fontugne, Global variations of the surface ocean productivity in low and mid latitudes: influence on $CO_2$ reservoirs of the deep ocean and the atmosphere during the last 21,000 years, *Paleoceanography* **3**, 361-399, 1988.

Shimmield, G. B., and N. B. Price, The scavenging of U, $^{230}$Th, and $^{231}$Pa during pulsed hydrothermal activity at 20°S, East Pacific Rise. *Geochim. Cosmochim. Acta* **52**, 669-677, 1988.

Shimmield, G. B., J. W. Murray, J. Thomson, M. B. Bacon. R. F. Anderson, and N. B. Price, The distribution and behaviour of $^{230}$Th and $^{231}$Pa at ocean margin, Baja California, Mexico, *Geochim. Cosmochim. Acta* **50**, 2499-2507, 1986.

Sholkovitz, E. R., H. Elderfield, R. Szymczak, and K. Casey, Island weathering: River sources of rare earth elements to the western Pacific ocean, *Mar. Chem.* **68**, 39-57, 1999.

Sholkovitz, E.R., The aquatic chemistry of rare earth elements in rivers and estuaries, *Aquatic Geochem.* **1**, 1-34, 1995.

Sholkovitz, E. R., The geochemistry of rare earth elements in the Amazon River estuary, *Geochim. Cosmochim. Acta* **57**, 2181-2190, 1993.

Siegenthaler, U., and J. L. Sarmiento, Atmospheric $CO_2$ and the ocean, *Nature* **365**, 119-125, 1993.

Sigman, D. M., and E. A. Boyle, Glacial/interglacial variations in the atmospheric carbon dioxide, *Nature* **407**, 859-869, 2000.

Stephens, M. P., and D. C. Kadko, Glacial-Holocene calcium carbonate dissolution at the central equatorial Pacific seafloor, *Paleoceanography* **12**, 797-804, 1997.

Stuiver, M., P. D. Quay, and H. G. Ostlund, Abyssal water carbon-14 distribution and the age of the world oceans, *Science* **219**, 849-851, 1983.

Suman, D. O., and Bacon M. P., Variations in Holocene sedimentation in the north American basin determined from $^{230}$Th measurements, *Deep Sea Res.* **36**, 869-878, 1989.

Thunell, R., D. Anderson, D. Gellar, and Q. Miao, Sea surface temperature estimates for the tropical western Pacific during the last glaciation and their implications for the Pacific warm pool",*Quat. Res.* **41**, 255-264, 1994.

Toggweiler, J. R., K. Dixon, and W. S. Broecker, The Peru upwelling and the ventilation of the South Pacific thermocline, *J. Geophys. Res.* **96** (C), 20467-20497, 1991.

Tomczak, M., and J. S. Godfrey, *Regional oceanography: an introduction*, Pergamon, Oxford, U.K., 442 pp., 1994.

Vincent, E., and W. H. Berger, Planktonic foraminifera and their use in Paleoceanography. In *The Sea*, Vol. 7, Emiliani, C. (Ed), Willey InterScience, New York, 1025-1119, 1981.

Walter, H. J., W. Geibert, M. M. Rutgers van der Loeff, G. Fischer, and U. Bathmann, Shallow vs. deep-water scavenging of $^{231}$Pa and $^{230}$Th in radionuclide enriched waters of the Atlantic sector of the Southern Ocean, *Deep Sea Res. A* **48**, 471-493, 2001.

Walter, H. J., M. M. Rutgers van der Loeff, and R. François, Reliability of the $^{231}$Pa/$^{230}$Th activity ratio as a tracer for bioproductivity of the ocean. In *Use of proxies in paleoceanography: Examples from the South Atlantic*, Fischer, G., and G. Wefer (Eds), Springer-Verlag, Berlin Heidelberg, Germany, 393-408, 1999.

Walter, H. J., M. M. Rutgers van der Loeff, and H. Hoeltzen, Enhanced scavenging of $^{231}$Pa relative to $^{230}$Th in the South Atlantic south of the Polar front: Implications for the use of the $^{231}$Pa/$^{230}$Th ratio as a paleoproductivity proxy, *Earth Planet. Sci. Lett.* **149**, 85-100, 1997.

Wefer, G., W. H. Berger, J. Bijma, and G. Fischer, Clue to ocean history: a brief overview of proxies. In *Use of proxies in paleoceanography: Examples from the South Atlantic*, Fischer, G., and G. Wefer (Eds), Springer-Verlag, Berlin Heidelberg, Germany, 1-68, 1999.

Yang, H.-S., Y. Nozaki, and H. Sakai, The distribution of $^{230}$Th and $^{231}$Pa in the deep-sea surface sediments of the Pacific Ocean, *Geochim. Cosmochim. Acta* **50**, 81-89, 1986.

Yu, E. F., R. François, and M. P. Bacon, Similar rates of modern and last-glacial ocean thermohaline circulation inferred from radiochemical data, *Nature* **379**, 689-694, 1996.

Yu, E. F., Variations in the particulate flux of $^{230}$Th and $^{231}$Pa and paleoceanographic applications of the $^{231}$Pa/$^{230}$Th ratio, Ph.D. thesis, MIT-WHOI, MA, U.S.A., 269 pp., 1994.

# Figures

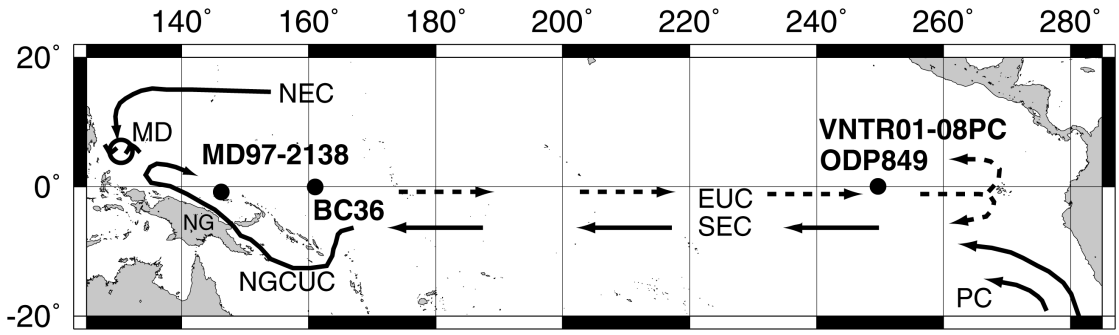


**Figure 1 - The equatorial Pacific Ocean, showing the location of the four cores analyzed (black circles): ODP 849 (leg 138, 0°11.59' N, 110°31.18' W, 3851 m water depth) and VNTR 8 (0°02.3' N, 110°28.5' W, 3800 m water depth) in the eastern equatorial Pacific, MD 2138 (1°25' S, 146°24' E, 1900 m water depth) in the western Pacific warm pool, and BC 36 (0° N, 161° E, 2311 m water depth) on the Ontong Java Plateau. The main currents are also represented: north equatorial current (NEC), equatorial undercurrent (EUC), south equatorial current (SEC), Peru current (PC), Mindanao Dome (MD) and New Guinea coastal undercurrent (NGCUC) originating from the SEC (Tomczak and Godfrey, 1994). NG indicates the island of New Guinea.**

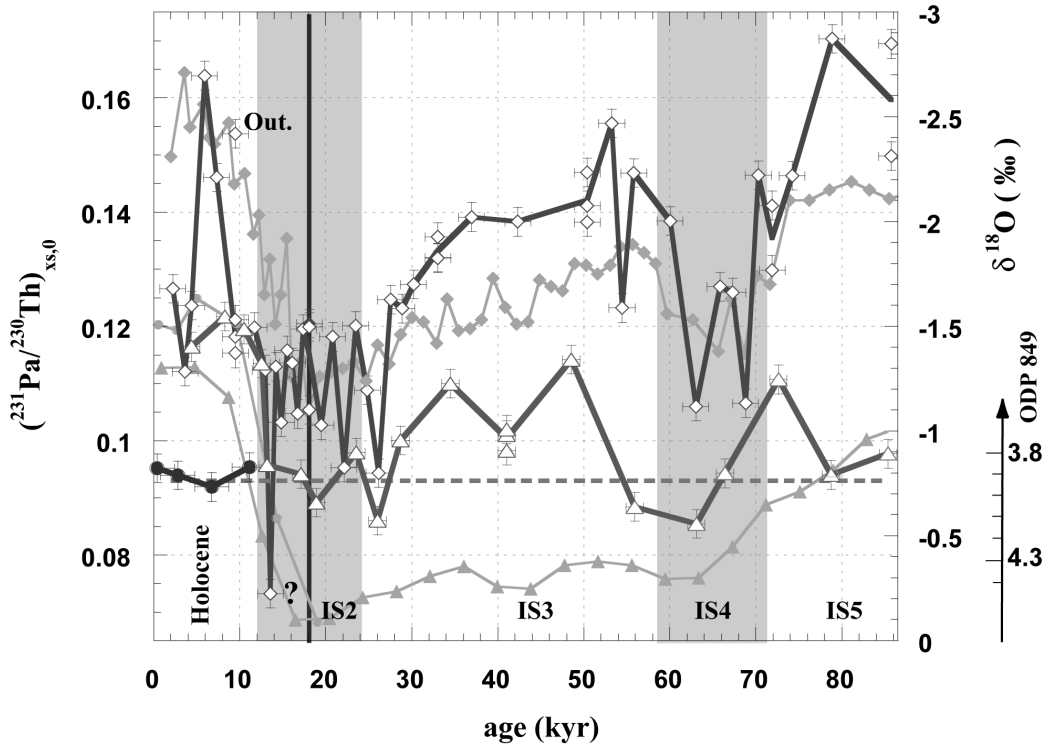


**Figure 2 - $(^{231}Pa/^{230}Th)_{xs,0}$ variations in three equatorial Pacific deep-sea sediment cores ODP 849 (open triangles), MD 2138 (open lozenges), and BC 36 (closed circles) over the last 86,500 years. Measurements were made by sector type ICP-MS. The production rate (0.093) is marked by a dashed horizontal line. The point in MD 2138 plotted with a question mark nearby is clearly out of the general trend. It is likely being an outlier. The point in MD 2138 plotted with an 'Out.' nearby is an outlier. It has been well identified since three replicates of this point show a $(^{231}Pa/^{230}Th)_{xs,0}$ ratio of 0.12, within 0.5 % (2σ level). The $\delta^{18}O$ records of the three cores are reported on the same graphic by light gray closed symbols and lines: ODP 849 (lozenges) (Mix et al., 1995), MD 2138 (triangles) (Beaufort et al., 2001), and BC 36 (circles) (Patrick and Thunell, 1997). Note that the scale is not the same for the ODP 849 $\delta^{18}O$ record. Glacial periods, corresponding to even numbered isotopic stages, i.e., IS 2 and IS 4 for this study, are shown in light gray. The LGM, around 18 kyr, is underlined by a vertical black line. The isotopic stage scale is from Imbrie et al. (1984).**

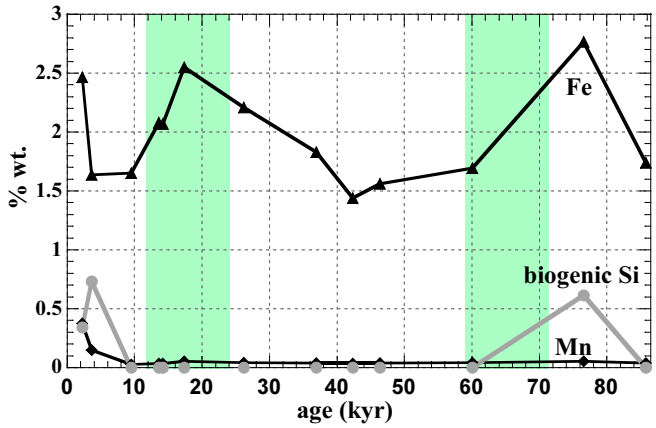


**Figure 3 - Biogenic Si (grey lozenges), Mn (black lozenges), and Fe (black triangles) content, expressed in % wt., in core MD 2138. Analyses were made by ICP-OES. Glacial periods are shown in light gray. Age boundaries are from Imbrie et al. (1984).**

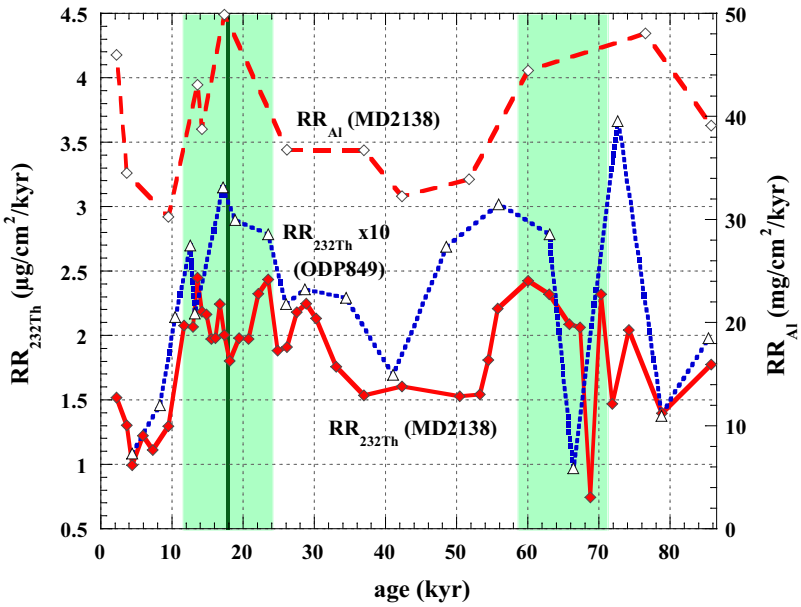


**Figure 4 - Al ($RR_{Al}$, open lozenges) and $^{232}Th$ ($RR_{232Th}$, closed lozenges) fluxes, normalized to $^{230}Th_{xs,0}$, in MD 2138 calculated after (2). The $^{232}Th$ flux ($RR_{232Th}$, open triangles) normalized to $^{230}Th_{xs,0}$ in ODP 849 is multiplied by 10 to fit the MD 2138 scale. Al and $^{232}Th$ fluxes units differ by a factor of $10^3$. The detrital flux varies the same way since both Al and $^{232}Th$ are proxies of continental material inputs. Glacial periods are shown in light gray. The LGM is marked with a vertical black line. Age boundaries are from Imbrie et al. (1984).**

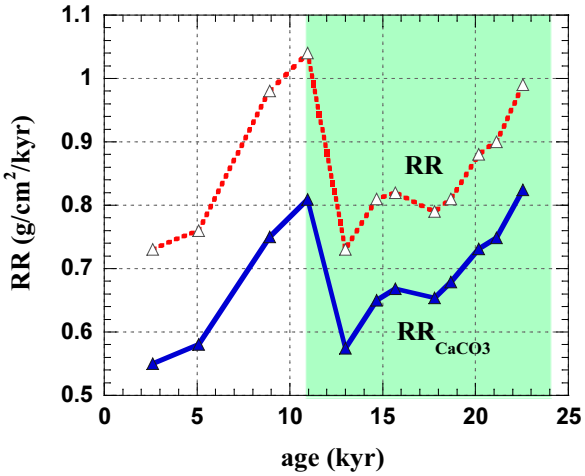


**Figure 5 - Total $^{230}Th_{xs,0}$ normalized flux (RR) calculated using (1) and carbonate $^{230}Th_{xs,0}$ normalised flux ($RR_{CaCO3}$) calculated using (2), in core VNTR01-08PC (0° N, 110° W). The carbonate content data (Snoecks and Rea, 1994) have been linearly interpolated to the ages (Mix, unpublished data) of our $^{230}Th_{xs,0}$ data in order to calculate the normalized flux. $^{230}Th_{xs,0}$ has been measured by α-spectrometry in VNTR01-08PC. The correlation coefficient between the two fluxes is 0.97, showing the control of the sedimentation by carbonate flux in the EEP. The last glacial period is shown in light gray. Age boundaries are from Imbrie et al. (1984).**

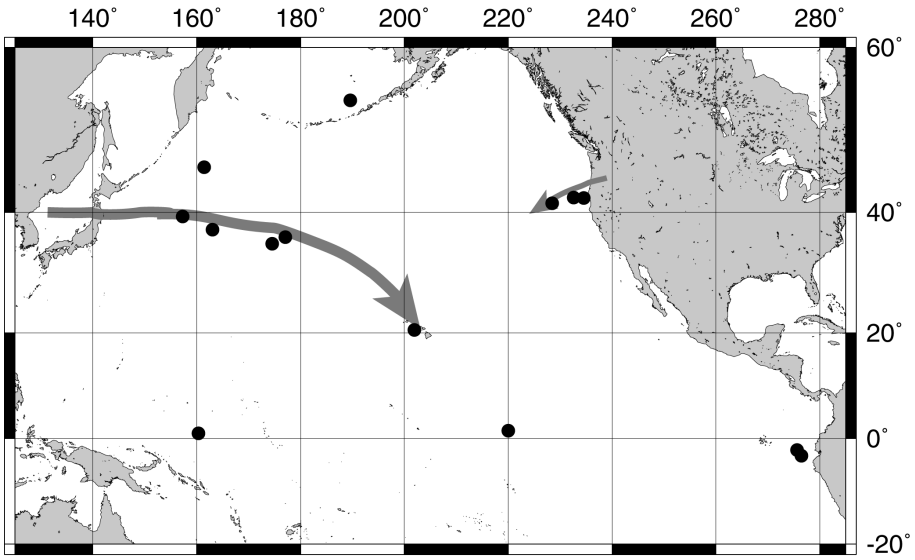


**Figure 6 - Location of the sediment cores (black circles) used by Lao et al. (1992b) and the main winds paths (gray arrows) that transport eolian dust to the Pacific. The gray arrow originating from Asia has been traced according to Merill et al. (1989) and the gray arrow originating from the Cascades Mountains, California has been traced according to Nakai et al. (1993). The two cores located on the East Pacific Rise from the study of Lao et al. (1992) have been removed.**

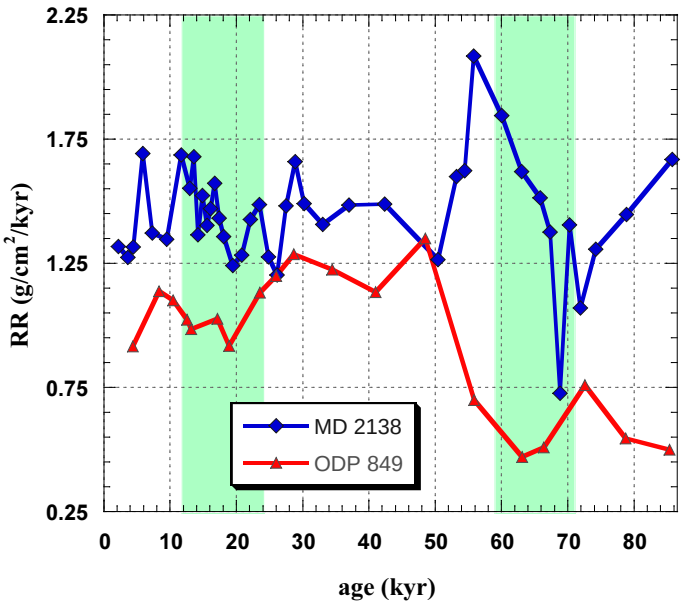


**Figure 7 - Total flux normalized to $^{230}Th_{xs,0}$ (RR) in core MD 2138 (1° N, 146° E) and core ODP 849 (0° N, 110° W) calculated using (1). Glacial periods are shown in light gray. Age boundaries are from Imbrie et al. (1984).**

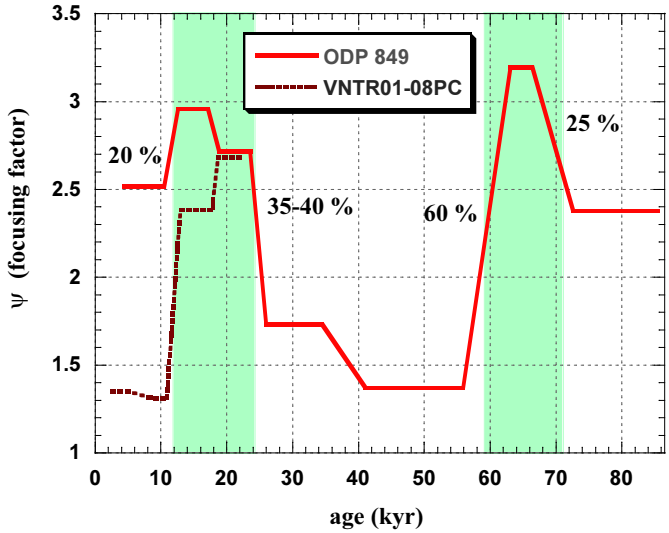


**Figure 8 - Sediment focusing factor ($\psi$) for core ODP 849 (0° N, 110° W) and ODP 849 site survey piston core VNTR01-08PC (0° N, 110° W) calculated using (3). $\psi > 1$ implies sediment focusing. In ODP 849, $\psi$ increases by a factor of 25 to 60 % during IS 2 and IS 4, compared with IS 3 and the end of IS 5. The decrease by a factor of 20 % between IS 2 and the Holocene is less significant. Glacial periods are shown in light gray. Age boundaries are from Imbrie et al. (1984).**

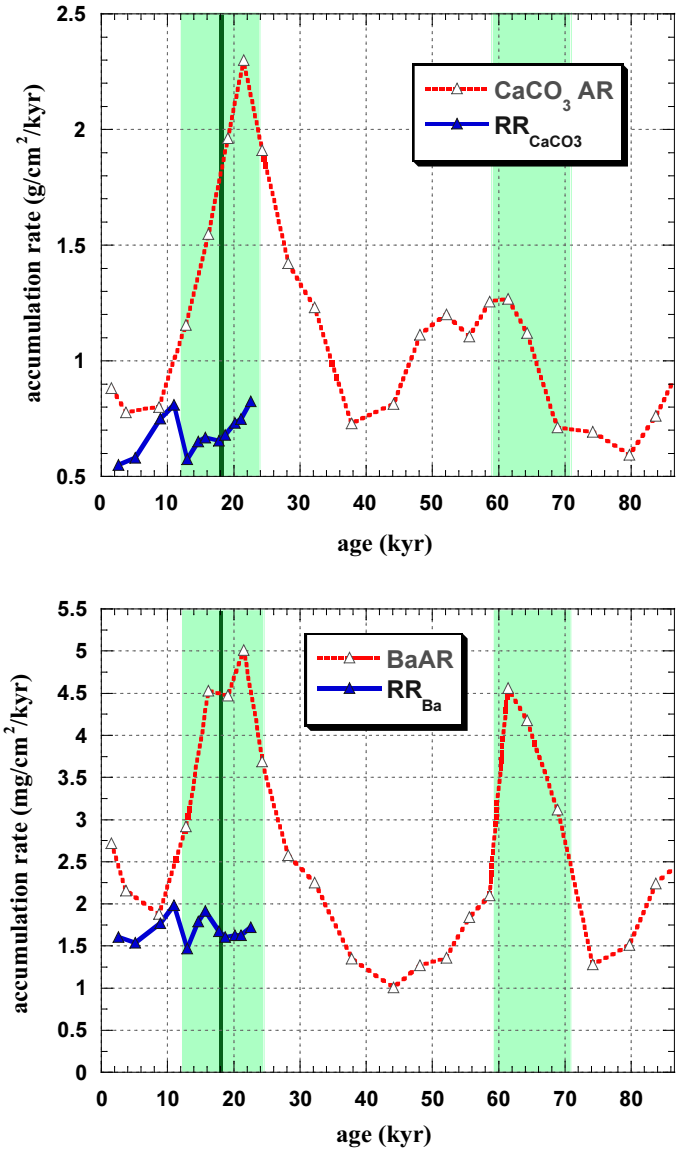


**Figure 9 - Down core carbonate (a) and barite (b) accumulation rates for VNTR01-08PC (0° N, 110° W). The $\delta^{18}O$ derived accumulation rate ((a) $CaCO_3AR$ and (b) BaAR) is equal to the $\delta^{18}O$ derived sediment mass accumulation rate (after Snoecks and Rea, 1994 and Mix, unpublished data) multiplied by the carbonate content (Snoecks and Rea, 1994) or the barite content (Paytan, 1995). The carbonate and the barite content data have been linearly interpolated to the ages (Mix, unpublished data) of our $^{230}Th_{xs,0}$ data in order to calculate the normalized flux ((a)RRCaCO3 and (b) $RR_{Ba}$) after (2). Glacial periods are shown in light gray. The LGM is marked with a vertical black line. Age boundaries are from Imbrie et al. (1984).**

# 7 - Origine des variations glaciaires/interglaciaires de la concentration atmosphérique de $CO_2$

Nos conclusions montrent que l'océan Pacifique équatorial n'a pas contribué à la réduction de la teneur en $CO_2$ de l'atmosphère. Au contraire, la diminution du pompage biologique, combinée à une intensification de la remontée d'eau au niveau de l'équateur, aurait augmenté le flux de $CO_2$ de l'océan vers l'atmosphère lors des périodes glaciaires par rapport à la période actuelle. Il n'est pas possible d'évaluer, sur la base de nos mesures, la quantité de $CO_2$ transférée de l'océan vers l'atmosphère par ce biais. Cependant, cet aspect devra être pris en compte dans les modèles qui reconstituent les variations de $CO_2$ atmosphérique entre les périodes glaciaires et interglaciaires.

En contrepartie, il doit donc exister une ou des zones où le transfert de $CO_2$ de l'atmosphère vers les océans est important lors des périodes glaciaires afin de pouvoir expliquer la baisse globale de 30 à 40 % de la teneur de $CO_2$ atmosphérique qui est enregistrée dans les carottes de glace (Neftel et al., 1983; Barnola et al., 1987; Raynaud et al., 1993; Petit et al., 1999).

L'utilisation du $\delta^{18}O$ atmosphérique, déduit de l'analyse des bulles d'air piégées dans la glace des pôles, comme proxy de la fonte des calottes glaciaires de l'hémisphère nord (Broecker and Henderson, 1998) permet de mettre en évidence que l'augmentation de la concentration atmosphérique en $CO_2$ précède la déglaciation dans l'hémisphère nord (figure 1) (Jouzel et al., 1993). Il en est de même pour la valeur du $\delta D$ (Jouzel et al., 1993). Ainsi, le réchauffement de l'Antarctique a eu lieu 8000 ans avant la fonte des calottes glaciaires dans l'hémisphère nord (Broecker and Henderson, 1998). De plus, l'augmentation de la pression partielle de $CO_2$ a lieu en même temps que la diminution des flux de poussières éoliennes (figure 1). Broecker and Henderson (1998) ont déterminé que cette diminution avait lieu (1) dans les sédiments marins de l'océan Antarctique, 4 kan avant la « Termination II » et (2) dans la calotte antarctique, 6 kan avant le milieu de la transition glaciaire/interglaciaire déterminée d'après le signal du $\delta^{18}O$ atmosphérique. La « Termination II » est déterminée par le milieu de la transition

glaciaire/interglaciaire dans le signal du $\delta^{18}O$ marin. Le temps de mélange atmosphérique de l'oxygène, qui est de 1 à 2 kan (Bender et al., 1994), est à l'origine de la différence de décalage temporel entre les données marines et les données des carottes de glace. Les changements de la circulation thermohaline dans l'Atlantique nord n'ont lieu que pendant ou après la déglaciation (Boyle and Keigwin, 1985; Oppo et al., 1997). Ils ne peuvent donc pas rendre être à l'origine de l'augmentation de la concentration atmosphérique en $CO_2$.

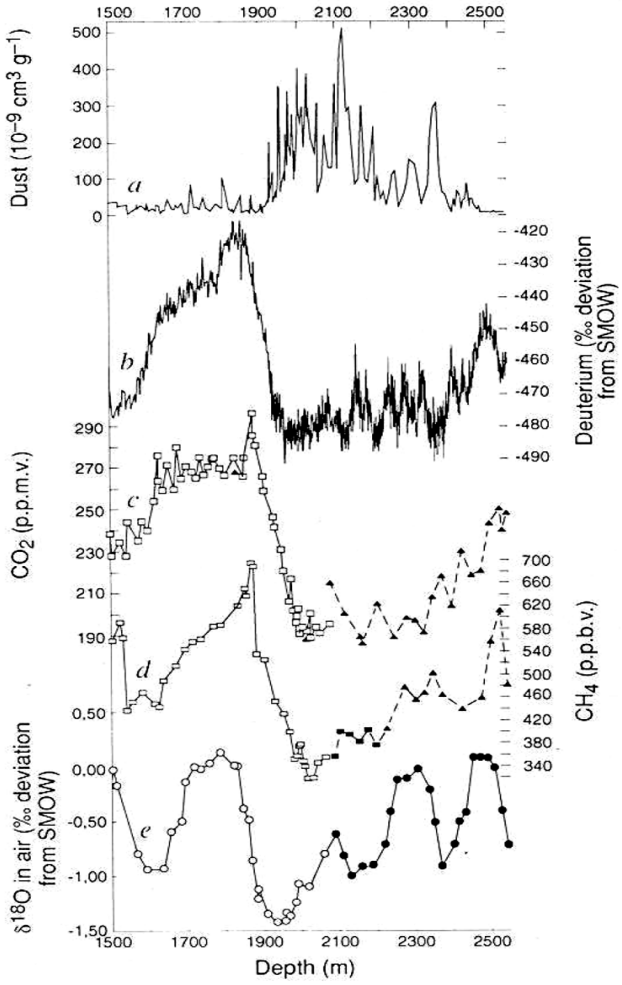


**Figure 10 - Données de la carotte de glace de Vostock, Antarctique. a, concentration en poussières éoliennes. b, concentration du deutérium, exprimée en déviation (‰) par rapport au standard SMOW. c, d, e, concentrations du $CO_2$, de $CH_4$, et de $\delta^{18}O$ de l'oxygène des bulles d'air piégées dans la glace. Jouzel et al. (1993).**

La corrélation entre le réchauffement de l'Antarctique, la diminution des flux de poussières au-dessus de la région antarctique et l'augmentation de la concentration atmosphérique du $CO_2$, montre que l'océan Antarctique joue un rôle majeur dans le

stockage du $CO_2$ et dans les variations glaciaires/interglaciaires de la concentration de ce gaz dans l'atmosphère. Cette région a déjà été proposée par plusieurs auteurs comme puits de $CO_2$ lors des périodes glaciaires (Knox and McElroy,1984; Martin, 1990; Siegenthaler and Sarmiento, 1993; François et al., 1997; Broecker and Henderson, 1998; Sigman and Boyle, 2000). Les principaux mécanismes proposés font essentiellement appel (1) à une augmentation de la productivité biologique qui augmenterait l'intensité de la pompe biologique de carbone et (2) à une stratification verticale de l'océan plus marquée, ce qui diminuerait le flux de $CO_2$ de l'océan vers l'atmosphère.

La plupart des modèles reconstituent les variations de $CO_2$ dans un océan en prenant en compte la variation globale de $CO_2$. Cependant, ces modèles devraient également considérer les variations en d'autres régions du globe, puisque, par exemple, notre étude permet de conclure que plus de $CO_2$ serait être injecté dans l'atmosphère au niveau de l'océan Pacifique équatorial lors des périodes glaciaires.

# Bibliographie

Barnola, J. M., D. Raynaud, Y. S. Korotkevich, and C. Lorius, Vostok ice core provides 160,000 year record of atmospheric $CO_2$, *Nature* **329**, 408-414, 1987.

Bender, M., T. Sowers, and L. Labeyrie, The Dole effect and its variations during the last 130,000 years as measured in the Vostok ice core, *Global Biogeochem. Cycles* **8**, 363-376, 1994.

Boyle, E.A., and L. D. Keigwin, Comparison of Atlantic and Pacific palaeochemical record for the last 250,000 years: Changes in deep ocean circulation and chemical inventories, *Earth Planet. Sci. Lett.* **76**, 135-150, 1985/1986.

Broecker, W. S., and G. M. Henderson, The sequence of events surrounding Termination II and their implications for the cause of glacial-interglacial $CO_2$ changes, *Paleoceanography* **13**, 352-364, 1998.

François, R. F., M. A. Altabet, E.-F. Yu, D. M. Sigman, M. P. Bacon, M. Frank, G. Bohrmann, G. Bareille, and L. D. Labeyrie, Water column stratification in the Southern Ocean contributed to the lowering of glacial atmospheric $CO_2$, *Nature* **389**, 929-935, 1997.

Henderson, G. M., and N. C. Slowey, Evidence against northern-hemisphere forcing of the penultimate deglaciation from U-Th dating, *Nature* **402**, 61-66, 2000.

Jouzel, J., N. I. Barkov, J. M. Barnola, M. Bender, J. Chapellaz, C. Genthon, V. M. Kotlyakov, V. Lipenkov, C. Lorius, J. R. Petit, D. Raynaud, G. Raisbeck, C. Ritz, T. Sowers, M. Stievenard, F. Yiou, and P. Yiou, Extending the Vostock ice-core record of palaeoclimate to the penultimate glacial record, *Nature* **364**, 407-412, 1993.

Knox, F., and M. McElroy, Changes in atmospheric $CO_2$: Influence of the marine biota at high latitudes, *J. Geophys. Res.* **89**, 4629-4637, 1984.

Martin, J. H., Glacial-Interglacial $CO_2$ change: The iron hypothesis, *Paleoceanography* **5**, 1-13, 1990.

Neftel, A., H. Oeschger, J. Schwander, B. Stauffer, and R. Zumbrunn, Ice core sample measurements give atmospheric $CO_2$ content during the past 40,000 yr, *Nature* **295**, 220-223, 1982.

Oppo, D., M. Horowitz, and S.J. Lehman, Marine core evidence for reduced deep water production during Termination II followed by a relatively stable MIS 5e (Eemian), *Paleoceanography* **12**, 51-63, 1997.

Petit, J. R., J. Jouzel, D. Raynaud, N. I. Barkov, J.-M. Barnola, I. Basile, M. Bender, J. Chappellaz, M. Davis, G. Delaygue, M. Delmotte, V. M. Kotlyakov, M. Legrand, V. Y. Lipenkov, C. Lorius, L. Pepin, C. Ritz, E. Saltzman, and M. Stievenar, Climate and atmospheric history of the past 420,000 years from the Vostock ice core, Antarctica, *Nature* **399**, 429-436, 1999.

Raynaud, D., J. Jouzel, J. M. Barnola, J. Chappellaz, R. J. Delmas, and C. Lorius, The ice record of greenhouse gases, *Science* **259**, 926-934, 1993.

Siegenthaler, U., and J. L. Sarmiento, Atmospheric $CO_2$ and the ocean, *Nature* **365**, 119-125, 1993.

Sigman, D. M., and E. A. Boyle, Glacial/interglacial variations in the atmospheric carbon dioxide, *Nature* **407**, 859-869, 2000.